

POLITECNICO DI TORINO

Collegio di Ingegneria Chimica e dei Materiali

**Corso di Laurea Magistrale
in Ingegneria Chimica e dei Processi Sostenibili**

Tesi di Laurea Magistrale

Prediction of flammable conditions of a methanol storage tank using Neural Networks.



Relatori

prof. Michaela Demichela
prof. Davide Fissore
ing. Gabriele Baldissoni

Candidato

Cristian Camilo Cañas Villegas

2021

Sommario

Introduzione

A causa della crescente domanda globale di energia e dello sviluppo industriale, le raffinerie, gli impianti chimici e le stazioni di distribuzione contengono grandi volumi di sostanze infiammabili. Molti di questi prodotti sono immagazzinati in serbatoi a temperatura ambiente e a pressione atmosferica. L'accensione di una miscela di sostanze infiammabili-aria all'interno di questi contenitori può portare ad esplosioni e il danno può variare da piccoli incidenti e qualche giorno di interruzione della produzione a incidenti maggiori con cause legali, crollo delle azioni o bancarotta dell'azienda (Chang and Lin, 2006).

La terza causa operativa più frequente di incidenti negli impianti chimici è dovuta allo stoccaggio. I serbatoi di stoccaggio a pressione atmosferica sono normalmente selezionati in base al punto di infiammabilità del liquido immagazzinato (Pouyakian *et al.*, 2021). Comunemente, gli oli non volatili come il diesel sono conservati in serbatoi con tetto a cupola; i liquidi volatili infiammabili come la benzina sono conservati in serbatoi con tetto galleggiante; e serbatoi orizzontali sono utilizzati nelle stazioni di servizio. Basato su un computo quantitativo, i serbatoi di stoccaggio con tetto a cupola e a tetto galleggiante sono i recipienti più pericolosi (Zheng and Chen, 2011).

Il metanolo è una delle materie prime più importanti nella chimica industriale. Tradizionalmente, è stato usato principalmente per la produzione chimica, sia come materia prima che come solvente (Dalena *et al.*, 2018). Il metanolo può essere immagazzinato in serbatoi a tetto fisso dotati di un sistema di inertizzazione (Methanol Institute, 2012).

L'inertizzazione o *gas blanketing* è una tecnica di prevenzione degli incendi e delle esplosioni che funziona riducendo la concentrazione di ossigeno in una miscela carburante-aria iniettando un gas inerte. In questo processo è necessario monitorare continuamente la concentrazione di ossigeno all'interno del serbatoio, questa misurazione può essere fatta per mezzo di un sensore in-situ (cioè, un sensore che viene inserito direttamente nel serbatoio). Questo sensore ha lo svantaggio che può dare misure sbagliate a causa della contaminazione del sensore e del fouling nella linea serbatoio-sensore (Nyce and Lipták, 2005).

Come alternativa alla misurazione continua dell'ossigeno, si possono usare alcuni metodi inferenziali. L'applicazione di questi metodi richiede un'analisi approfondita del processo/impianto per garantire che sia sempre raggiunta l'inertizzazione, poiché non esiste una misurazione diretta del livello di ossigeno.

Recentemente, i modelli basati sulle reti neurali sono utilizzati per risolvere diversi problemi come il riconoscimento di pattern, il backup dei sistemi di misurazione, l'analisi *what-if*, la predizione in tempo reale per il controllo degli impianti, la convalida dei sensori e le strategie di diagnosi dei guasti. Una rete neurale è un processore distribuito in parallelo composto da unità di elaborazione semplici (neuroni) che hanno una propensione naturale per immagazzinare apprendimento esperienziale e renderlo disponibile per l'uso (Fortuna *et al.*, 2001).

L'obiettivo di questo lavoro è lo sviluppo di un soft sensor basato su reti neurali per la previsione della concentrazione di vapore all'interno di un serbatoio di metanolo dotato di un sistema di inertizzazione. Conoscere le concentrazioni dei vapori all'interno del serbatoio permette di identificare situazioni pericolose e garantire il funzionamento in sicurezza dell'impianto, il

monitoraggio con sensori fisici non è sempre possibile a causa di limitazioni economiche e sfide tecniche, e la previsione con modelli dinamici richiede una conoscenza approfondita del sistema. Si propone di utilizzare una rete neurale per la previsione delle concentrazioni. Le reti neurali sono modelli computazionali che permettono la modellazione di sistemi senza informazioni precedenti perché hanno la capacità di imparare addestrandosi con esempi, in più, a causa delle loro connessioni parallele permettono alte velocità di trasmissione di informazione e risposta quasi immediata, che li rende i candidati perfetti per operare in tempo reale. Inoltre, si distinguono per la loro facilità di implementazione e di accoppiamento con la tecnologia esistente.

Per raggiungere questo obiettivo, in primo luogo è stato sviluppato il modello matematico del serbatoio partendo da principi fenomenologici e facendo alcune considerazioni per facilitare la sua implementazione in Matlab. Una volta verificato il comportamento del sistema a diversi impulsi, è stata valutata la superficie di risposta delle condizioni di infiammabilità del sistema a variazioni casuali di diverse ampiezze nelle variabili di ingresso. Successivamente, vengono proposte quattro configurazioni di *soft sensor* basate in modelli di reti neurali che vengono addestrate e testate con due set di dati diversi ottenuti attraverso il modello matematico. Ogni configurazione viene testata e viene selezionata quella con le migliori prestazioni. Infine, il *soft sensor* scelto viene testato ulteriormente per valutare la sua performance in una situazione in cui si raggiungono condizioni di infiammabilità all'interno del serbatoio. È stato trovato che la configurazione del *soft sensor* con le migliori prestazioni è la configurazione B, la quale ha il maggior numero di variabili di input, questa configurazione è in grado di prevedere in modo soddisfacente le concentrazioni nel serbatoio anche quando il sistema entra in condizioni di infiammabilità.

Materiali e metodologie utilizzate

Descrizione del serbatoio di stoccaggio

Un serbatoio di stoccaggio verticale con un tetto fisso e una capacità di 100 m^3 è considerato come caso di studio. Il serbatoio è stato progettato per immagazzinare il metanolo necessario per un processo, permettendo un flusso costante e garantendo la disponibilità del reagente in ogni momento. La figura sottostante mostra il disegno del serbatoio con le principali linee di ingresso e di uscita.

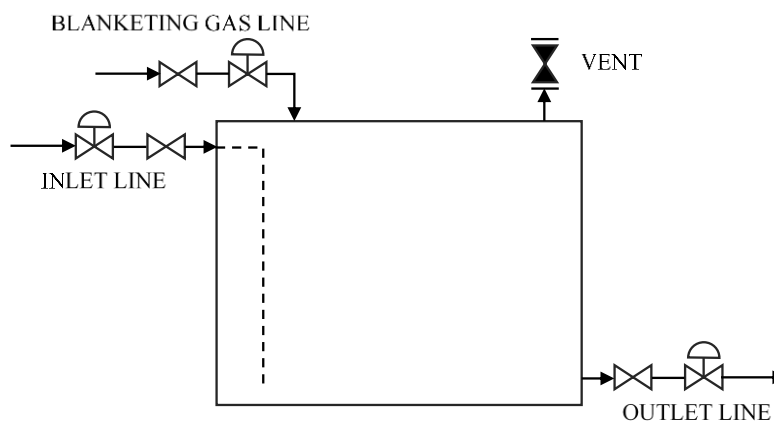


Figura 0.1: Disegno del serbatoio di metanolo.

La geometria del serbatoio è cilindrica, ha un tetto piatto e funziona a pressione atmosferica. I componenti principali del serbatoio sono:

- *Linea di ingresso:* permette il riempimento del serbatoio, consiste in un tubo situato nella parte superiore del serbatoio e si estende fino a pochi centimetri prima del fondo del serbatoio.
- *Linea di uscita:* permette l'estrazione della sostanza attraverso una pompa, si trova sul fondo del serbatoio
- *Linea di gas blanketing:* Fornisce l'azoto che aiuta ad evitare la formazione di un'atmosfera esplosiva all'interno del serbatoio
- *Sfiato:* Dispositivo meccanico progettato per fornire il rilascio della pressione o del vuoto.

Come accennato sopra, lo scopo del serbatoio è quello di fornire una costante alimentazione di metanolo. Da un lato, il metanolo viene estratto attraverso la linea di uscita e alimentato al processo attraverso un sistema di tubi e pompe. D'altra parte, quando il livello del liquido è inferiore al 30% della capacità totale del serbatoio, la fase di riempimento procede, e il metanolo viene alimentato fino a quando il livello del serbatoio raggiunge l'80%.

A causa delle restrizioni e dei pericoli dello stoccaggio del metanolo, il sistema ha una linea di azoto che aiuta a compensare la caduta di pressione dovuta allo svuotamento, evita l'ingresso di aria e il raggiungimento delle condizioni di esplosività.

La valvola di sfiato permette di mantenere la pressione vicino al valore atmosferico permettendo ai vapori di uscire dallo spazio di testa o all'aria di entrare a seconda che il sistema sia pressurizzato o in condizioni di vuoto. I valori di set point della valvola di sfiato sono stati stabiliti secondo i criteri per i serbatoi di stoccaggio di metanolo proposti da Bechtold (1997).

Il set point della concentrazione di ossigeno per questo serbatoio è definito come due punti percentuali sotto la concentrazione limite di ossigeno (LOC) come raccomandato dal CEN (2006).

Procedura seguita

In primo luogo, il modello matematico del serbatoio è stato generato utilizzando le equazioni descritte nella sezione 2.1. Per risolvere il sistema di equazioni differenziali, è stato utilizzato il solver-ODE23 incorporato in Matlab. Dato che non ci sono dati sperimentali per convalidare il modello matematico, viene fatta soltanto una verifica che il modello funzioni correttamente e risponda come previsto, a questo scopo il sistema viene alimentato con input di tipo gradino nelle variabili di ingresso e viene osservata la risposta del serbatoio al fine di confermare il comportamento atteso e la relazione tra le variabili.

È stata studiata la risposta nelle coordinate di infiammabilità del sistema a un input casuale di ampiezza massima definita. Gli intervalli di variazione per F2 e F3 sono stati del 20%, 40%, 60% e 80% per ciascuno di essi. L'algoritmo descritto nella sezione 2.6. è stato utilizzato per generare un set di dati con un'estensione di 300.000 punti per ogni variazione dell'ampiezza dell'input. Sono stati generati un totale di otto set di dati, uno per ciascun intervallo di variazione. Successivamente, ognuno dei set di dati è stato presentato al modello matematico che restituisce il valore di tutte le variabili del sistema in ogni momento. Con le concentrazioni nello spazio di testa, si calcolano le

coordinate di infiammabilità e si plottano i risultati. L'obiettivo di questo test è quello di determinare l'intervallo minimo di variazione per ogni variabile che potrebbe generare una situazione di rischio nel sistema.

Viene selezionato l'intervallo di F2 e F3 in cui il sistema esplora le condizioni vicine alla penisola di infiammabilità. Successivamente viene creato un nuovo set di dati di input di 45.000 punti con una variazione casuale e contemporanea di F2 e F3, che viene alimentato al modello matematico. Tutti i valori delle variabili del sistema vengono salvati e costituiscono il database per l'addestramento delle reti neurali. I dati di test sono ottenuti in modo analogo cambiando i range di variazione e la lunghezza del *dataset*.

È stato utilizzato un set di quattro diversi *layout*, per determinare quale presenta le migliori prestazioni (**Figura 0.2**), in ogni configurazione sono state utilizzate diverse reti neurali. Nella sezione 2.3 si presenta informazione più dettagliata delle reti neurali utilizzate.

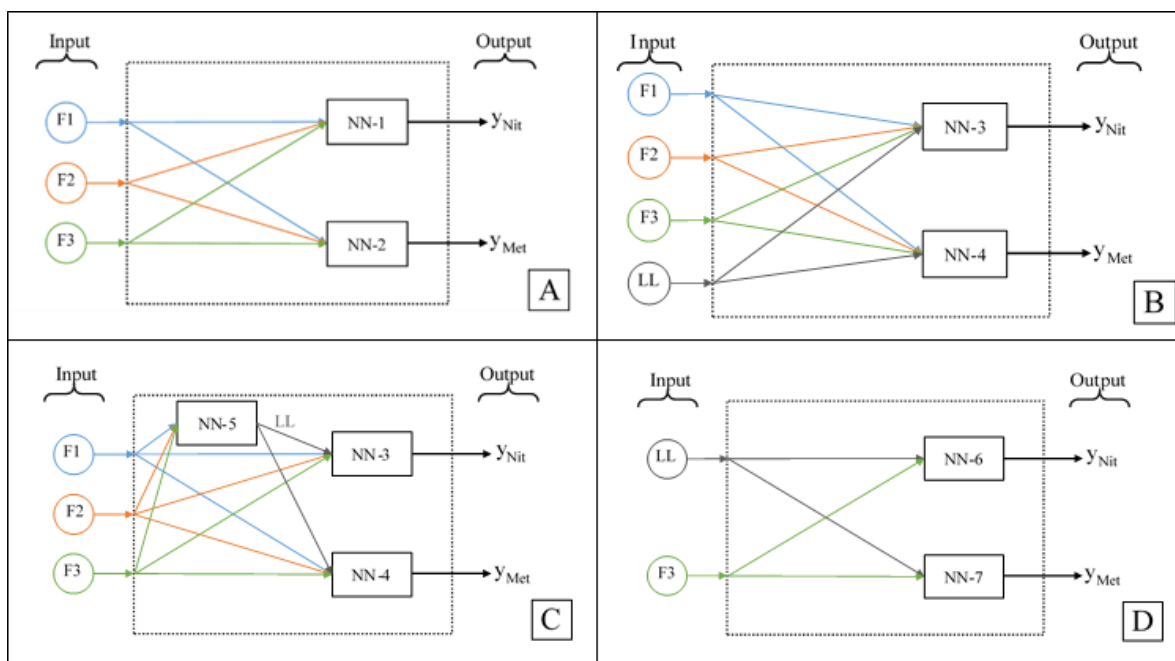


Figura 0.2: Set di configurazioni proposti come *soft sensor*.

Le reti neurali sono state create ed addestrate utilizzando l'algoritmo presentato nella sezione 2.4. Le coppie input-output sono state selezionate in base alla rete da addestrare e i valori presi dal database creato in precedenza. Successivamente, le prestazioni di tutte le reti neurali sono state valutate utilizzando il medesimo database di prova. La migliore configurazione è stata scelta in base a due criteri: l'errore quadratico medio e il confronto grafico tra la risposta prevista per le reti neurali e quella attesa.

Infine, il *layout* con le migliori prestazioni viene selezionato come *soft sensor* proposto e viene ulteriormente testato per valutare il comportamento del sensore virtuale in una situazione in cui il sistema entra in condizioni infiammabili.

*Risultati e discussione.***Risposta del sistema a variazioni a gradino**

Si valuta il comportamento del sistema a variazioni a gradino negli ingressi. Quando la portata di uscita di metanolo (F2) è aumentata del 30% del suo valore stazionario si osserva un aumento della concentrazione di ossigeno e una diminuzione della concentrazione di azoto, mentre la concentrazione di metanolo rimane approssimativamente costante. Al contrario, quando il valore di F2 è diminuito, la frazione di metanolo rimane costante, mentre la frazione di azoto aumenta e quella di ossigeno diminuisce.

Nel caso di variazioni nel flusso di azoto (F3) mantenendo il flusso di uscita di metanolo costante si osserva che la concentrazione di ossigeno varia inversamente al variare di F3, cioè diminuisce all'aumentare del F3. Mentre la concentrazione di azoto varia direttamente con F3.

In tutti gli scenari valutati, si osserva che dopo il completamento del processo di riempimento, la concentrazione di azoto aumenta, ma le concentrazioni di metanolo e ossigeno diminuiscono temporaneamente. Questo può essere spiegato perché durante il riempimento il volume disponibile per i vapori diminuisce generando un aumento della pressione, se questa è superiore al set point dello sfiato i gas vengono rilasciati. Alla fine della fase di riempimento la quantità di gas è ridotta, e il serbatoio è leggermente pressurizzato, poiché il flusso di azoto e l'uscita di metanolo si mantengono costanti, si verifica un aumento della concentrazione di azoto. Con il passare del tempo, la pressione si recupera e la variazione delle concentrazioni presenta un comportamento simile a quello osservato prima del riempimento.

La concentrazione all'interno del serbatoio dipende dai valori di F2 e F3 in quanto F3 deve essere impostato per recuperare la pressione persa quando il serbatoio viene svuotato. Quando il valore di F3 non è in grado di mantenere la pressione, si genera una situazione di vuoto e si permette l'ingresso di aria, con conseguente aumento della concentrazione di ossigeno. Inoltre, quando si verifica la situazione opposta, cioè quando c'è un flusso di F3 superiore a quello richiesto per bilanciare la caduta di pressione, si genera una situazione di sovrappressione e i vapori possono uscire, con una conseguente diminuzione del contenuto di ossigeno. La frazione di metanolo rimane approssimativamente costante perché dipende principalmente dalla pressione di saturazione del metanolo.

Risposta del sistema a un input casuale.

La superficie di risposta delle condizioni d'infiammabilità si rappresenta in un diagramma di tipo cartesiano con gli assi definiti secondo le **Equazione 0.1** e **0.2**. Questo tipo di diagramma fu proposto per Casal (2008) e permette di rappresentare graficamente i processi di inertizzazione.

$$x = \frac{\text{Volme inerte}}{\text{Volume infiammabile}} * 100 \quad (0.1)$$

$$y = \frac{\text{Volume infiammabile} + \text{Volme inerte}}{\text{Volume Totale (inflammabile + inerte + aria)}} * 100 \quad (0.2)$$

Le condizioni di infiammabilità all'interno del serbatoio sono state valutate quando le variabili F2 e F3 sono variate casualmente nel tempo entro i range: 20%, 40%, 60% e 80%. Come previsto, all'aumentare dell'intervallo di variazione, la superficie di risposta aumenta, si osserva che il sistema raggiunge le condizioni di infiammabilità solo quando la variazione di F2 o F3 è nell'intervallo dell'80%. Lo studio della risposta del sistema viene considerato come base per definire i range di variazione del set di apprendimento.

Per la creazione del set di dati di apprendimento delle reti neurali, il serbatoio viene simulato per 7500 h e viene usato un range di variazione pari all'80% per F2 e F3. La risposta delle condizioni di infiammabilità del sistema all'input del dataset di apprendimento è mostrata nella **Figura 0.3**. Si osserva che combinando l'effetto delle due variabili la superficie di risposta del sistema è aumentata, in questo caso entra più profondamente nella penisola dell'infiammabilità.

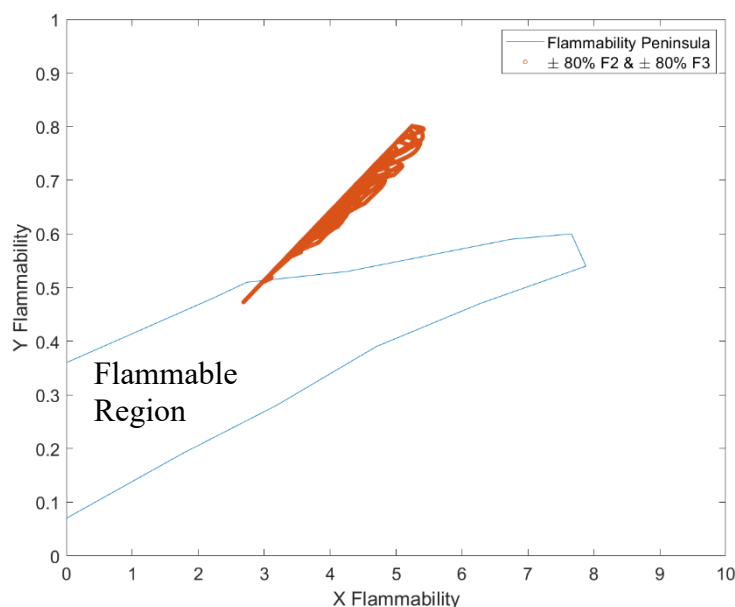


Figura 0.3: Diagramma di infiammabilità per il set de dati di addestramento. La linea blu rappresenta la penisola d'infiammabilità, mentre i punti arancione la risposta del sistema all'input di addestramento.

Valutazione di diverse configurazioni di *soft sensor*.

La **Tabella 0.1** presenta l'errore quadratico medio (MSE) per la previsione ottenuta con le reti neurali addestrate quando viene presentato il set di dati utilizzato per l'apprendimento.

Tabella 0.1: MSE calcolato per la previsione delle reti neurali per il set di apprendimento.

	SETUP-A	SETUP-B	SETUP-C	SETUP-D
MSE y_{Met} prediction	1.2E-07	4.6E-09	1.5E-06	1.1E-06
MSE y_{Nit} prediction	5.0E-06	2.9E-07	5.4E-07	3.4E-05

Il minor MSE è stato ottenuto con il setup B che ha F1, F2, F3 e LL come input, mentre la rete neurale con il più alto errore è stata D che ha come input LL e F3. Questo indica che la presenza di ingressi aggiuntivi ha un effetto positivo sulle prestazioni della rete. Per garantire che il fenomeno dell'*overtraining* non sia presente e per valutare la previsione della dinamica del sistema, viene eseguito un ulteriore test con tutte le reti addestrate

La **Tabella 0.2** mostra il riassunto dell'errore quadratico medio per ogni configurazione quando è stato utilizzato il set di dati di test. Rispetto alla **Tabella 0.1**, si può notare che gli errori calcolati per il set di prova sono dell'ordine di grandezza, o vicini, all'errore ottenuto con il set di apprendimento, indicando che l'addestramento della rete neurale è stato fatto correttamente e che non è presente *overtraining*.

Tabella 0.2: MSE calcolato per la previsione delle reti neurali per il set di prova.

	SETUP-A	SETUP-B	SETUP-C	SETUP-D
MSE y_{Met} prediction	2.4502e-07	3.2991e-08	1.8116e-06	8.2038e-07
MSE y_{Nit} prediction	9.5963e-06	7.5037e-07	8.4823e-07	1.7221e-04

Si osserva che in tutti i casi valutati (Sezione 3.3), il sistema presenta i residui più alti nelle zone vicine al riempimento del serbatoio, una possibile ragione per spiegare questo è il fatto che è in questa zona dove si verificano i maggiori cambiamenti nella concentrazione del sistema.

Quando si confrontano i risultati ottenuti con il setup A e il setup B, si conclude che la presenza di informazioni aggiuntive sul livello aiuta a migliorare le prestazioni della rete, questo è dimostrato sia dall'analisi grafica che dai risultati MSE ottenuti. Tuttavia, nel setup C, che utilizza gli stessi input del setup A (F1, F2, F3) e predice internamente il livello nel serbatoio, si osserva un incremento dell'errore per la previsione delle concentrazioni rispetto a quelle ottenute con il setup B, il che può indicare che la rete neurale utilizzata per la previsione del livello presenta errori nel suo output che vengono amplificati nella previsione della frazione di metanolo.

Il Setup B viene selezionato per la prova finale in base alla risposta grafica osservata e al valore MSE ottenuto per il set di apprendimento e il set di test.

Risultati del test finale.

Il Setup B è selezionato per eseguire il test finale e verificare le sue prestazioni prevedendo le concentrazioni quando il sistema entra in condizioni di infiammabilità. La figura sottostante mostra i risultati ottenuti, il riquadro blu mostra i valori di input forniti al *soft sensor*, mentre quello arancione mostra il confronto tra il valore ottenuto con il modello fenomenologico e il valore previsto dalla rete neurale. Per le condizioni valutate il sensore soft può predire in modo soddisfacente le concentrazioni.

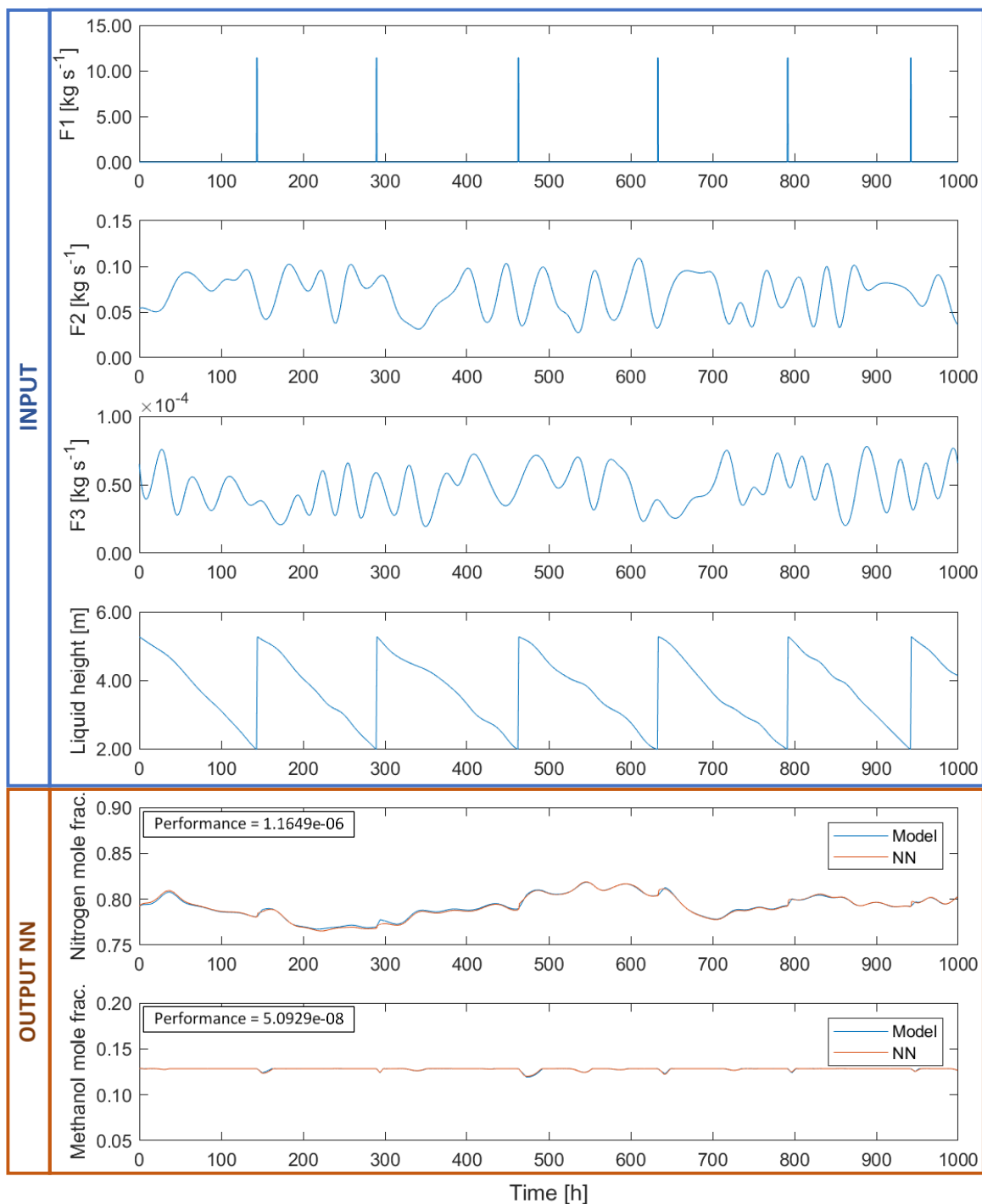


Figura 0.4: Risultati test finale

La **Figura 0.5** mostra la variazione temporale della frazione di ossigeno prevista dal modello matematico e la confronta con il valore calcolato a partire dalle previsioni delle concentrazioni di metanolo e azoto riportate nella precedente figura. Come previsto anche in questo caso il sistema predice in modo soddisfacente la concentrazione di ossigeno, essendo in grado di prevedere anche quando il sistema è in condizioni di infiammabilità.

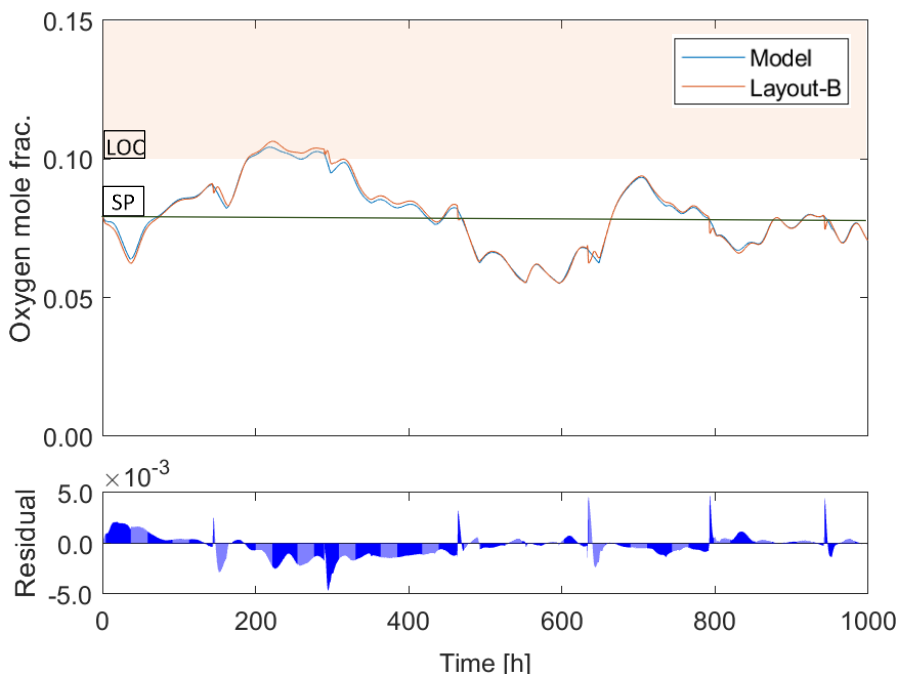


Figura 0.5: Risultati test finale concentrazione ossigeno.

Conclusioni

È stato possibile progettare un soft sensor in grado di prevedere la concentrazione all'interno di un serbatoio di stoccaggio di metanolo con sistema di inertizzazione dell'azoto, le migliori prestazioni sono state ottenute utilizzando come variabili di input il flusso di ingresso e di uscita del metanolo, il flusso di azoto, e il livello del liquido all'interno del serbatoio. Il sensore soft utilizza un modello Neural-Network-NARX, ed è stato addestrato utilizzando dati ottenuti attraverso il modello matematico.

Le reti neurali differiscono dai modelli fenomenologici perché sono modelli matematici basati sul funzionamento del cervello e possono essere addestrati per modellare un sistema senza conoscere le leggi fisiche che lo sottendono. Durante il processo di apprendimento la rete neurale regola i suoi parametri interni, il che le permette di adattarsi e trovare le relazioni esistenti tra le variabili. Questa caratteristica adattiva dà alle reti neurali un vantaggio rispetto al modello matematico tradizionale.

Il processo di definizione dell'architettura della rete è un processo di prova ed errore, poiché non ci sono regole prestabilite per impostarla, tuttavia, alcune regole empiriche che rendono questo compito un po' più facile possono essere trovate nella letteratura. In questo caso tutte le reti neurali utilizzate consistono in un singolo *hidden layer*. Di solito, un singolo *hidden layer* di neuroni è sufficiente per le situazioni di interesse, tuttavia, per problemi impegnativi con dinamiche complesse è possibile utilizzare più di uno strato.

L'applicazione dei risultati del presente lavoro è limitata dalla capacità del modello matematico di rappresentare adeguatamente il sistema reale. Quando si sviluppa un modello fenomenologico che rappresenta un sistema fisico, si fanno delle semplificazioni perché non tutte le informazioni

del sistema da rappresentare sono sempre note. La validità di queste semplificazioni deve essere verificata con i dati sperimentali.

Tra le possibili applicazioni del sensore virtuale sviluppato nel presente lavoro si possono trovare:

- Previsione della concentrazione in tempo reale.
- Sensore di backup.
- Allarme di sicurezza

La procedura utilizzata nel presente lavoro per ottenere il *soft sensor* è versatile e può essere applicata in molteplici applicazioni e attrezzature diverse, soprattutto in quelle in cui la sperimentazione con dispositivi reali non è possibile a causa di limitazioni di sicurezza o economiche.

TABLE OF CONTENTS

LIST OF FIGURES.....	iii
LIST OF TABLES	v
1. Introduction.....	1
1.1. Flammability.....	3
1.1.1. Flammability limits.....	3
1.1.2. Flash point temperature.....	3
1.1.3. Autoignition temperature.....	3
1.2. Inertization.....	3
1.2.1. Inertization Methods.....	4
1.2.2. Specifications of safe limits.....	5
1.2.3. Flammability diagram.....	6
1.2.4. x-y Diagram.....	7
1.3. Methanol.....	8
1.4. Soft Sensor Design.....	10
1.5. Neural Networks.....	12
1.5.1. Network architecture.....	13
1.5.2. Activation function.....	15
1.5.3. Learning processes.....	16
1.5.4. Use NN for Real-time estimation for monitoring and control.....	18
1.5.5. Nonlinear autoregressive exogenous model (NARX).....	18
2. Materials and methods.....	21
2.1. Description of the storage tank.....	21
2.2. Mathematical model of the storage tank.....	22
2.2.1. Calculation of time invariant parameters.....	28
2.3. Soft Sensor design.....	29
2.3.1. Layout A.....	29
2.3.2. Layout B.....	30
2.3.3. Layout C.....	30
2.3.4. Layout D.....	31
2.4. Neural networks description.....	31
2.5. Dataset generation.....	33
2.6. Input random generation.....	33

- 2.7. Procedure followed.....35
- 3. Results and discussion.....37
 - 3.1. Response of the system to a step function.....37
 - 3.2. Response of the system to a random input.42
 - 3.3. Evaluation of different soft sensor setups.....44
 - 3.4. Final test performance.50
 - 3.5. Final Remarks.....52
- 4. Conclusions.54
- References55
- List of symbols and abbreviations.....58
 - List of symbols.....58
 - List of abbreviations.....59
- Acknowledgments60
- Appendix A: Matlab code - Creation and training NARX Neural network.....61
- Appendix B: Matlab code - Input Random Generation63

LIST OF FIGURES

Figure 1.1: Operation processes involved at the time of accidents. Adapted from Zheng and Chen (2011)	1
Figure 1.2: Nitrogen blanketing system. Adapted from Nyce and Lipták (2005)	2
Figure 1.3: Specification of safe limits for control. Adapted from Baldissin (2015).	6
Figure 1.4: Ternary Flammability diagram. Adapted from Mashuga and Crowl (1998)	7
Figure 1.5: x-y Flammability diagram.	8
Figure 1.6: Methanol production expressed in mln ton per year of production from 1975 to 2016. Adapted from Dalena et al. (2018).	8
Figure 1.7: World methanol demand from 2006 to 2016. Adapted from Dewey Johnson (2012). ..	9
Figure 1.8: Flammability envelope for methanol. Taken from Brooks and Crowl (2007).	9
Figure 1.9: Flammability diagram in Cartesian coordinates for methanol.	10
Figure 1.10: Graphical representation of a soft sensor.	10
Figure 1.11: Typical steps for the development of a soft sensor. Adapted from (Fortuna et al., 2007).	11
Figure 1.12: Stereotyped representation of a biological neuron	12
Figure 1.13: Graphical representation of an artificial neuron.	13
Figure 1.14: Single layer, fully connected neural network.	14
Figure 1.15: Fully connected feedforward network with one hidden layer and one output layer. ..	14
Figure 1.16: Recurrent network	15
Figure 1.17: Block diagram of learning with a teacher, the part of the figure printed in blue constitutes a feedback loop.	16
Figure 1.18: Architectures of the NARX neural network	19
Figure 2.1: Methanol storage tank.	21
Figure 2.2: Flow diagram for the methanol tank.	23
Figure 2.3: Soft sensor Layout A.	30
Figure 2.4: Soft sensor Layout B.	30
Figure 2.5: Soft sensor Layout C.	31
Figure 2.6: Soft sensor Layout D.	31
Figure 2.7: Procedure followed for the creation and training of the neural network.	32
Figure 2.8: Random vector generation example.	34
Figure 2.9: Procedure followed for the development of the soft sensor.	36
Figure 3.1: Response of the tank when a step in F2 equal to +30% of the steady state value at time = 50 h is applied. The orange vertical bar is used to indicate the filling time of the tank.	38
Figure 3.2: Response of the tank when a step in F2 equal to -30% of the steady state value at time = 50h is applied. The orange vertical bar is used to indicate the filling time of the tank.	39
Figure 3.3: Response of the tank when a step in F3 equal to +30% of the steady state value at time = 50 h is applied. The orange vertical bar is used to indicate the filling time of the tank.	40
Figure 3.4: Response of the tank when a step in F3 equal to -30% of the steady state value at time = 50 h is applied. The orange vertical bar is used to indicate the filling time of the tank.	41
Figure 3.5: Variation of flammability conditions inside the tank for a random input in time of F2 keeping F3 constant.	42
Figure 3.6: Variation of flammability conditions inside the tank for a random input in time of F3 keeping F2 constant.	43
Figure 3.7: Flammability diagram for the learning set using in the network training.	43

Figure 3.8: Data set for overtraining evaluation.	45
Figure 3.9: Concentration of methanol predicted by setup A.	46
Figure 3.10: Concentration of Nitrogen predicted by setup A.....	46
Figure 3.11: Concentration of Methanol predicted by setup B.....	47
Figure 3.12: Concentration of Nitrogen predicted by setup B.	47
Figure 3.13: Concentration of Methanol predicted by setup C.....	48
Figure 3.14: Concentration of Nitrogen predicted by setup C.....	48
Figure 3.15: Concentration of Methanol predicted by setup D.....	49
Figure 3.16: Concentration of Nitrogen predicted by setup D.....	49
Figure 3.17: Concentration of nitrogen and methanol predicted by setup B wen the input showed is presented to the network.....	51
Figure 3.18: Concentration of oxygen calculated from the prediction of the neural network.	52

LIST OF TABLES

Table 2.1: Methanol tank dimensions and operative conditions	22
Table 2.2: List of variables and nomenclature.	24
Table 2.3: Invariant parameters.....	27
Table 2.4: DOF Analysis.....	27
Table 2.5: Antoine Equation parameters. Data from NIST.....	29
Table 2.6: Density Equation parameters. Data from (Coker, 2010).....	29
Table 2.7: Neural networks used in the soft sensor.....	33
Table 3.1: MSE calculated for the prediction of the trained neural networks for the learning set.	44
Table 3.2: Performance of the neural network's configurations evaluated when test is presented.	50

1. Introduction.

Due to the increasing global energy demand and industrial development, refineries, chemical plants and distribution stations contain large volumes of flammable substances. Many of these products are stored in tanks at normal temperatures and atmospheric pressure. The ignition of a flammable substance-air mixture within these containers can lead to explosions and the damage can range from small accidents and a few days of production interruption to major accidents in lawsuits, stock devaluation, or company bankruptcy (Chang and Lin, 2006).

According to Tauseef *et al.* (2018) 97% of all fuel tank accidents involve flammable chemicals. Furthermore, Chang and Lin (2006) reviewed 242 accidents that occurred in the last decades related to atmospheric and pressurized tanks that contained oil or chemicals and found that 60% of these accidents were fires and 25% explosions.

As shown in **Figure 1.1**, the third most frequent operating cause of accidents was due to storage. Atmospheric pressure storage tanks are normally selected based on the flash point of the stored liquid (Pouyakian *et al.*, 2021). Commonly, nonvolatile oils such as diesel are stored in dome-roof tanks, volatile flammable liquids such as gasoline are stored in floating roof storage tanks, horizontal tanks are used in gas stations. Based on a numerical count, dome-roof and floating roof storage tanks are at the top two of most dangerous vessels (Zheng and Chen, 2011).

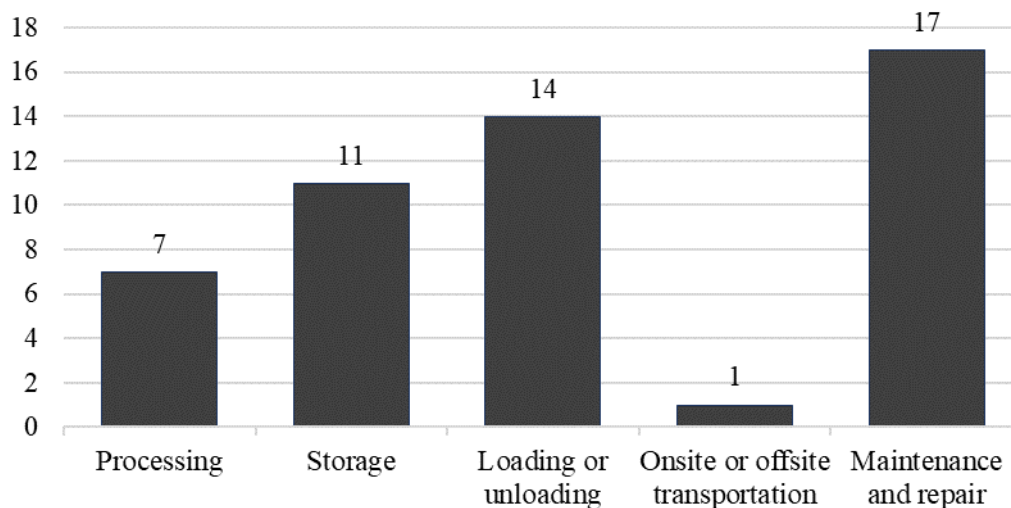


Figure 1.1: Operation processes involved at the time of accidents. Adapted from Zheng and Chen (2011)

Methanol is one of the most important commodities in industrial chemistry. Traditionally, the primary uses of methanol have been for chemical production, as either a feedstock or a solvent or cosolvent. Nowadays, it is considered one of the most useful chemical compounds (Dalena *et al.*, 2018). Methanol can be stored in fixed roof tanks provided of a gas blanketing system (Methanol Institute, 2012). Inertization or gas blanketing is a fire and explosion prevention technique that works by reducing the oxygen concentration in a fuel-air mixture by injecting an inert gas (**Figure 1.2**). In this process it is necessary to continuously monitor the oxygen concentration inside the tank, and the measurement can be done by means of an in-situ sensor (i.e., a sensor which is inserted

directly into the vessel). This sensor has the disadvantage that can give wrong measurements because of the contamination of the sensor and the fouling in the tank-sensor line (Nyce and Lipták, 2005).

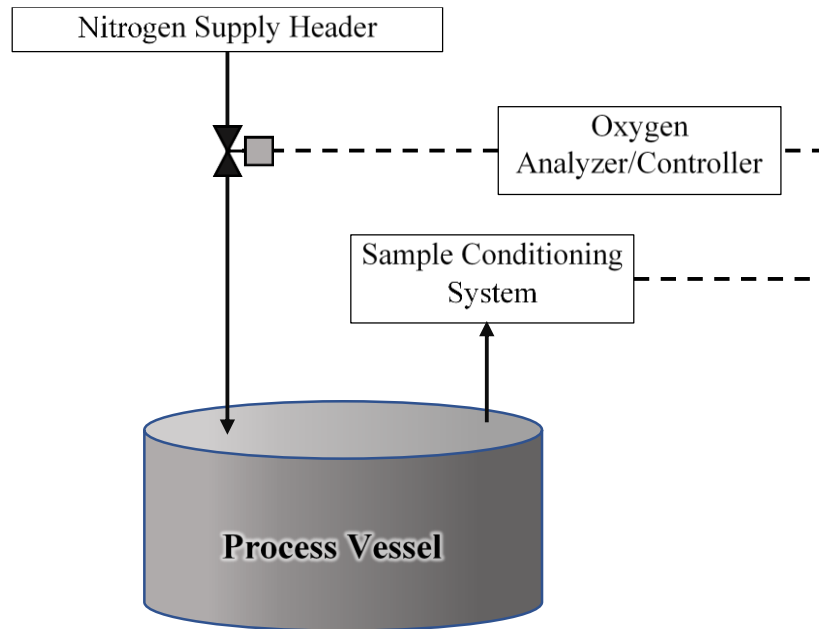


Figure 1.2: Nitrogen blanketing system. Adapted from Nyce and Lipták (2005)

As an alternative to continuous oxygen measurement, some inferential methods can be used. The application of these methods requires a thorough analysis of the process/plant to ensure that adequate inerting is always achieved as there is no direct measurement of the oxygen level.

Recently, neural network-based models are used to solve several different problems such as pattern recognition, measuring system back-up, what-if analysis, real-time prediction for plant control, sensor validation and fault diagnosis strategies. A neural network is a massively parallel distributed processor made up of simple processing units (neurons) that has a natural propensity for storing experiential knowledge and making it available for use (Fortuna *et al.*, 2001).

In this work, a soft sensor is presented for estimating the concentration of vapors inside a fixed roof methanol storage tank equipped with a nitrogen inerting system. Knowing the vapor concentrations inside the tank allows to identify hazardous situations and always ensure the safe operation of the system. A neural network is proposed to be used for concentration prediction because they allow modeling of systems without prior information and can be operate in real time prediction. This soft sensor is built using a neural network model and trained using the data obtained through a phenomenological model of the fuel tank. Both the neural network and the tank model were developed using Matlab®.

1.1. *Flammability.*

Flammable substances or mixtures are grouped according to their physical characteristics into gases, liquids, solids, and aerosols. The flammability risk level for a flammable liquid depends mainly on three parameters: flammability limits, flash temperature and autoignition temperature. Based on the value of these parameters, different substances can be handled more easily than others, e.g., diesel burn less easily than gasoline, and therefore are easier to handle.

1.1.1. Flammability limits.

Mixtures of a flammable gas or vapor with air are flammable only in a certain range of concentrations, this range is delimited by the lower flammability limit (LFL) and by the upper flammability limit (UFL) (Baldissin, 2015). Below the LFL in the presence of an ignition source flame propagation does not occur, as the gas concentration is not sufficient to sustain the flame. Above the UFL the mixture does not have enough oxygen to allow the flame to spread (Carson and Mumford, 2002). The presence of inert substances in the system can reduce the oxygen concentration, and then modify the flammability features of a substance.

Flammability limits are commonly expressed in percent by volume of the fuel at 25°C. The LFL is probably the most important limit since it is directly related to the formation of flammable atmospheres (Casal, 2008).

1.1.2. Flash point temperature.

Flash temperature is the minimum temperature at which a flammable liquid, under certain test conditions, produces enough vapors to form a flammable mixture. The flash point temperature is an essential parameter to determine the dangerousness of a flammable liquid in terms of fire risk.

Flammable liquids are classified according to the European Chemicals Agency (2017) into:

- Category 1. - Liquids whose vapors can give rise to explosion: Flash point < 23 °C and initial boiling point ≤ 35 °C.
- Category 2. - Flammable liquids: Flash point < 23 °C and initial boiling point > 35 °C.
- Category 3. - Combustible liquids: Flash point ≥ 23 °C and ≤ 60 °C.

1.1.3. Autoignition temperature.

Autoignition temperature is the minimum temperature, at atmospheric pressure, at which a fuel in contact with air burns spontaneously without the need for an external heat source. At this temperature, sufficient activation energy is reached to start the combustion reaction (Casal, 2008).

1.2. *Inertization.*

During the storage of flammable substances, flammable atmospheres can be generated inside fuel storage tanks, when a sufficient amount of energy is supplied to the mixture, it may be ignited and lead to either or both an explosion and a fire (Taveau, 2011). An example of the formation of

flammable mixtures is the emptying of a tank, when the level of the stored liquid begins to drop, the volume of the vapors increases generating a drop in the pressure, to prevent the collapse of the tank and report the pressure to atmospheric conditions the entry of air is allowed, depending on the amount of air entering and the concentration of the fuel vapors, flammable conditions can be reached. One way to control the oxygen concentration in the headspace is by introducing an inert substance, commonly nitrogen. This technique is known as inerting or gas blanketing.

1.2.1. Inertization Methods.

Methods of inertization applying nitrogen fall into five primary configurations and are dependent on the needs and logistics of the actual process being controlled, these methods assume perfect back-mixing of the headspace vapors (Methanol Institute, 2017).

Method 1 - Continuous pressurized purging or manual pressure control.

To ensure adequate protection against the formation of flammable atmospheres inside the tank, the pressure of the headspace gas should be kept slightly above atmospheric pressure. This protection pressure is selected considering economic and technical criteria. In order to avoid unnecessary loss of gas, the working pressure is normally chosen below the vent pressure (CEN, 2006).

In continuous purge, nitrogen is introduced into the tank as a continuous flow exits through a vent. This method consumes a large volume of inert gas, increases fuel loss due to evaporation, and does not always reliably maintain an inert atmosphere. A pressure reducing valve (PRV) is used to blanket the tank (Methanol Institute, 2017).

Method 2 - Automatic pressure control.

This protection method consists of the automatic control of the pressure inside the tank. It is applicable in industries with a digital control system (DCS). In its most basic configuration, the DCS detects the pressure inside the tank and manipulates the opening of the nitrogen valve. In some cases, it is possible to manipulate the ventilation valve to allow the gases to escape and reduce the pressure of the system.

This type of system is usually more expensive than the continuous purging method because it has a greater number of components. However, it allows a more precise control and has the advantage of being able to perform alarm or control functions in response to overpressure or under-pressure conditions.

Method 3 - Oxygen control

This method uses an oxygen analyzer to measure the oxygen concentration inside the vessel, the control system uses this measurement to change the flow of nitrogen into the tank. By directly measuring the headspace concentration, efficient use of nitrogen is achieved, and non-flammability conditions are always guaranteed.

The oxygen analyzer is located at the upper part of the tank and is connected to it through a pipe. The implementation of this system is expensive because both the equipment and the

installation are expensive, in addition, periodic maintenance of the analyzer lines and their sensor calibration is required (Nyce and Lipták, 2005).

Method 4 - Dual Control: Oxygen and pressure.

Some processes require precise control of headspace conditions to guarantee the quality of the final products. It is possible, in these cases, to use a control system that manipulates the nitrogen flow based on the simultaneous measurement of the pressure and the headspace concentration. Combining the two measurements prevents the entry of air in the process of emptying the tank.

This method is the most expensive to implement and requires a higher degree of complexity in programming logic. However, it allows a very strict control and a high efficiency in the use of nitrogen (Methanol Institute, 2017).

Method 5 - Other variable control.

As an alternative to measuring oxygen concentration and pressure, other variables can be measured, such as moisture content. This method like Method 2 and Method 3 allows an efficient use of nitrogen.

1.2.2. Specifications of safe limits.

During the normal operation of processes or equipment equipped with inerting systems, fluctuations in oxygen concentration may occur. To guarantee the formation of non-explosive atmospheres, it is necessary to constantly measure the oxygen content and ensure that it is below the limiting oxygen concentration (LOC). Generally, there are four values of oxygen concentrations to observe (**Figure 1.3**):

- limiting oxygen concentration (LOC).
- maximum allowable oxygen concentration (MAOC) in the equipment.
- trip point (TP), at which the process controller initiates a shut-down trip.
- set point (SP), at which the process controller maintains the oxygen concentration.

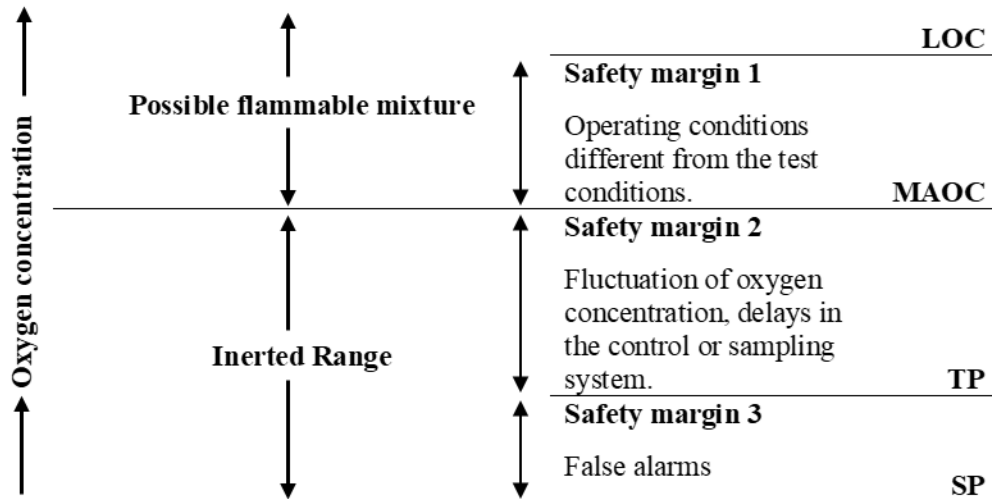


Figure 1.3: Specification of safe limits for control. Adapted from Baldissin (2015).

The limiting oxygen concentration or minimum oxygen concentration is defined as the limiting concentration of oxygen, independent of the concentration of fuel, below which combustion is not possible (JOIFF, 2015). The LOC value is determined by standardized tests under specified temperature and conditions. The MAOC of the process is obtained by calculation the LOC at the process conditions.

When the concentration reaches the trip point the controller begins to shut down to put the equipment in safety. There must be a sufficient margin of operability between the TP and the MAOC to allow the control system to bring the equipment to safety without reaching flammable conditions.

The set point concentration depends on the MAOC value and the type of concentration monitoring (CEN, 2006):

Where the oxygen concentration is continuously monitored, a safety margin of at least 2 volume percentage points below the MAOC should be maintained, unless the MAOC is less than 5%, in which case the oxygen concentration should be maintained at no more than 60% of the MAOC. Where the oxygen concentration is not continuously monitored, the oxygen concentration should be maintained at less than 60 % of the MAOC, unless the MAOC is less than 5%, in which case the oxygen concentration should be maintained at less than 40% of the MAOC.

1.2.3. Flammability diagram.

A very useful tool to determine if a mixture of gas and vapors is flammable is through a flammability diagram. The two most used diagrams are the triangular diagram and the x-y diagram.

Triangular Flammability diagram

The **Figure 1.4** shows a typical triangular flammability diagram, it can be used to represent all the possible mixtures of the three components of the system (Fuel-Oxygen-Nitrogen).

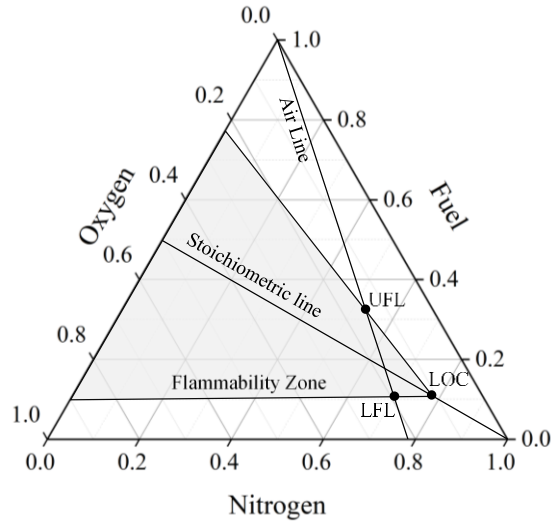


Figure 1.4: Ternary Flammability diagram. Adapted from Mashuga and Crowl (1998)

This diagram gives us the following information:

- *Flammability zone:* is the region of the diagram in which all mixtures are flammable.
- *Air line:* represents all possible concentrations of fuel and air. The intersections of the air line with the flammability envelope are the LFL and UFL.
- *The stoichiometric line:* represents all the possible stoichiometric combinations of fuel and oxygen.
- *Limiting oxygen concentration (LOC)* or minimum oxygen concentration.

1.2.4. x-y Diagram.

Another way to represent the flammability is present in the **Figure 1.5**. Using a Cartesian diagram is possible to facilitate the graphical representation of the inerting procedures (Casal, 2008). Here the axes are defined as:

$$x = \frac{\text{Inert volume}}{\text{Flammable volume}} * 100 \quad (1.1)$$

$$y = \frac{\text{Flammable volume} + \text{Inert volume}}{\text{Total volume (Flammable + Inert + Air)}} * 100 \quad (1.2)$$

In this graph, the origin ($x = 0, y = 0$) represents the condition where the entire vapor phase is composed only by air. The flammability envelope interceptions with y-axis represent the LFL and UFL.

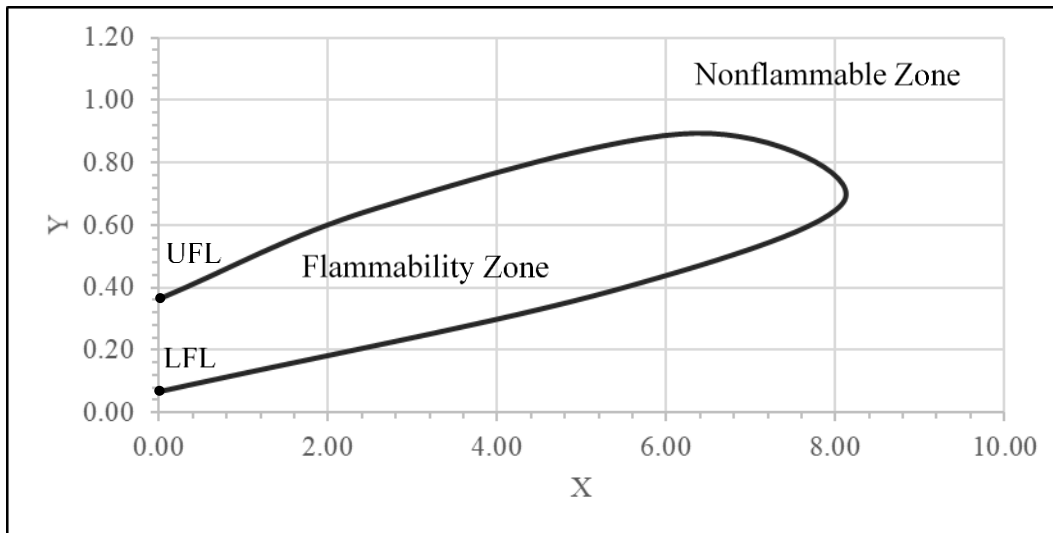


Figure 1.5: x-y Flammability diagram.

1.3. Methanol.

One of the most widely used flammable liquids is methanol or methyl alcohol: it is an organic compound, CH_3OH , with a molecular weight equal to 32.042 u.m.a. At ambient conditions is a colorless, neutral, polar, and flammable liquid. It is miscible with water, alcohols, esters, and most other organic solvents. It is only slightly soluble in fats and oils. Other common names for methanol include methyl alcohol, methyl hydrate, wood spirit, wood alcohol, and methyl hydroxide (Ott et al., 2012).

Originally, methanol was produced by destructive distillation of wood. Nowadays, methanol can be produced from several carbon-containing feedstocks, such as natural gas, coal, biomass, and CO_2 (Zhen and Wang, 2015). The **Figure 1.6** shows the methanol production from 1975 to 2016.

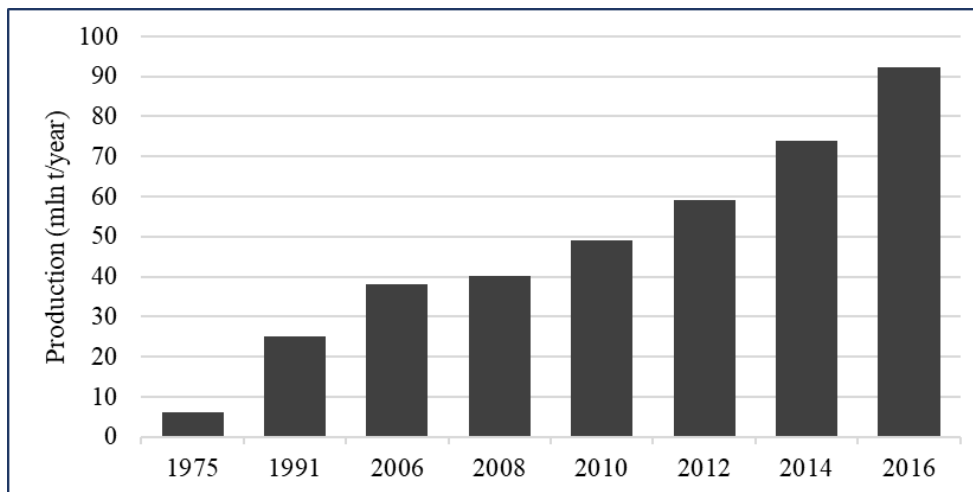


Figure 1.6: Methanol production expressed in mln ton per year of production from 1975 to 2016. Adapted from Dalena et al. (2018).

Methanol is one of the most innovative and versatile molecules and is used as a building block for many chemicals and products. Other uses include windshield washer antifreeze, fuels, wastewater treatment and biodiesel production (Methanex, 2006). Recently, new fuel/energy applications for methanol are emerging, increasing the demand. The **Figure 1.7** shows the demand of methanol from 2006 to 2016.

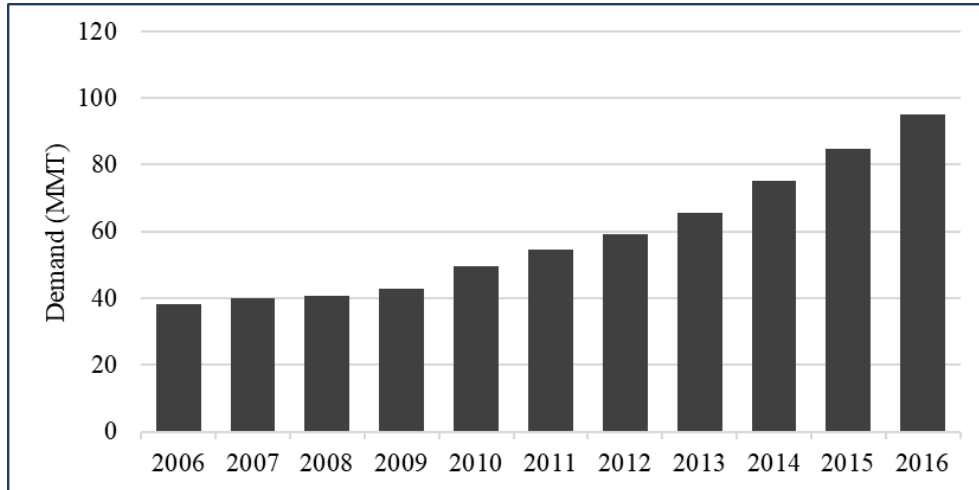


Figure 1.7: World methanol demand from 2006 to 2016. Adapted from Dewey Johnson (2012)

As methanol demand and production increases, there is a need for more available storage. The guidelines for designing, fabricating, constructing, repairing, and safeguarding methanol storage tanks are similar to those used for gasoline. However, the unique characteristics of methanol make necessary to take additional precautions (Methanol Institute, 2012). One of the main characteristics of methanol is its range of flammability, its UFL is 36% (Brooks and Crowl, 2007). The **Figure 1.8** shows the flammability envelope for methanol.

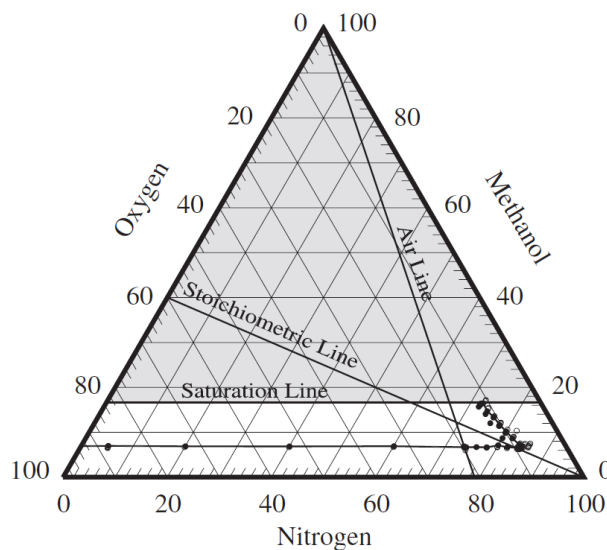


Figure 1.8: Flammability envelope for methanol. Taken from Brooks and Crowl (2007).

Taking the data reported by Brooks and Crowl (2007) it is possible to construct the flammability diagram in Cartesian coordinates (**Figure 1.9**).

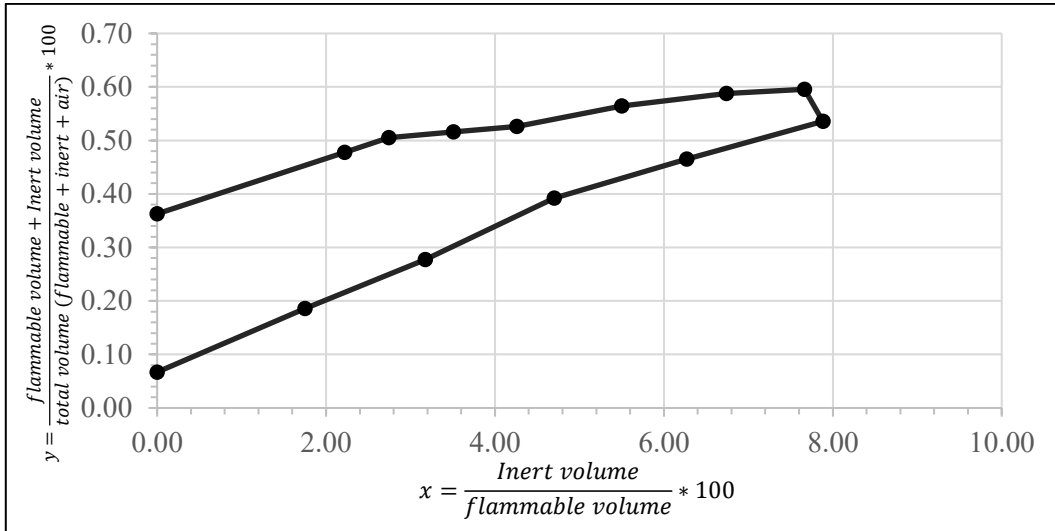


Figure 1.9: Flammability diagram in Cartesian coordinates for methanol.

To prevent the formation of explosive atmospheres inside the tanks, inert gas blanketing is frequently used, and dry nitrogen is the preferred inert gas. To protect the tank from overpressure or under-pressure vents are normally used (Methanol Institute, 2017).

1.4. Soft Sensor Design.

A soft sensor is the name given to a software that focuses on the estimation of some system variable using mathematical models and the data acquired by other physical sensors available in the system (**Figure 1.10**).

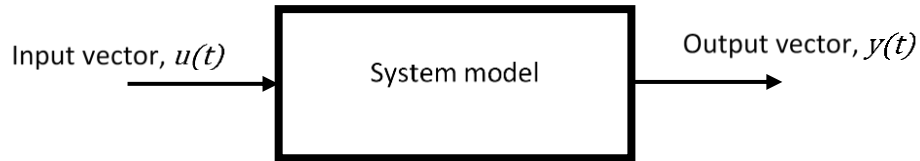


Figure 1.10: Graphical representation of a soft sensor.

The typical steps for the development of a soft sensor are shown in **Figure 1.11**; however, the procedure is not a linear task and many times some parts of the design must be reconsidered.

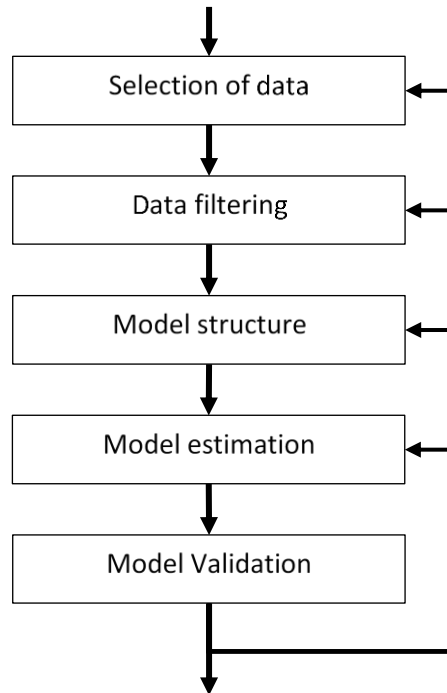


Figure 1.11: Typical steps for the development of a soft sensor. Adapted from (Fortuna et al., 2007).

The first step in soft sensor development is to identify the variables that can influence the response of the soft sensor and the availability of the data. In industrial applications, plant databases are normally used to store historical measurements of process variables obtained with analog sensors.

The data collected in the plant database are generally corrupted by the presence of outliers, so it is necessary to perform a data filtering process, where different techniques can be applied. An unfiltered dataset used in the model estimation may result in a poor model performance that is not able to represent the dynamics of the system.

The structure of the final model is determined from a set of proposed models. Among the most used types of models are: Neural Networks, Linear models, polynomial models, and neuro-fuzzy models. In this step it is of vital importance to know the dynamics of the system since the model candidates will have a better or worse performance depending on the relationship between the input and output variables.

Once the best model has been selected, the next step is to find the parameters that ensure the best performance (Tunning). This is done through criteria established by the designer. The minimization of the mean square error (MSE) between the actual value of the system and its estimate output is commonly used.

The final step is model validation, in which it is verified that the model can adequately represent the underlying system. A general rule to follow in sensor validation is to use a different dataset than the one used in the model estimation stage to avoid overfitting, i.e., the situation when the sensor can represent adequately the learning set but performs poorly with a different dataset. Graphical representations can be powerful tools for model validation.

It is important to emphasize that in all the steps of the soft sensor design it is necessary to have expert personnel who know well the operation and dynamics of the system, since they can be of great help especially when selecting the relevant variables, delays, sampling time, operating range, nonlinearity of the system and in the identification of the errors in the historical records.

1.5. Neural Networks.

Artificial neural networks (ANN) or simply neural networks (NN) are a mathematical/computational model inspired by the functioning of biological neural networks. Gurney (1997) defines NN as:

A neural network is an interconnected assembly of simple processing elements, units or nodes, whose functionality is loosely based on the animal neuron. The processing ability of the network is stored in the interunit connection strengths, or weights, obtained by a process of adaptation to, or learning from, a set of training patterns.

The stereotyped representation of a biological neuron is presented in **Figure 1.12**. This is constituted of dendrites, axon and a central body also called soma which contains the cell nucleus inside. The nucleus adds the input signals coming from the synapse and arriving through the dendrites, when the signal reaches a threshold value the neuron produces an output signal that travels through the axon which, in turn is connected with dendrites from neighboring neurons.

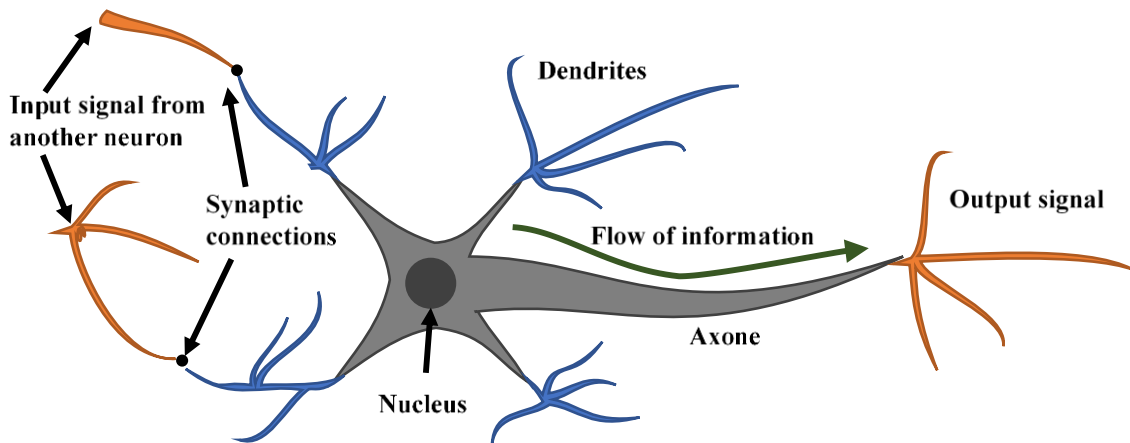


Figure 1.12: Stereotyped representation of a biological neuron

The **Figure 1.13** shows the graphical model of an artificial neuron. The input signals are the stimuli that the neuron receives from its surroundings, each input has an associated weight that represents its relative importance and is modified in the learning process. The summing function performs the summation of the weighted inputs and adds a bias term. Lastly, the resulting signal is fed to an activation function that determines the value of the neuron's output.

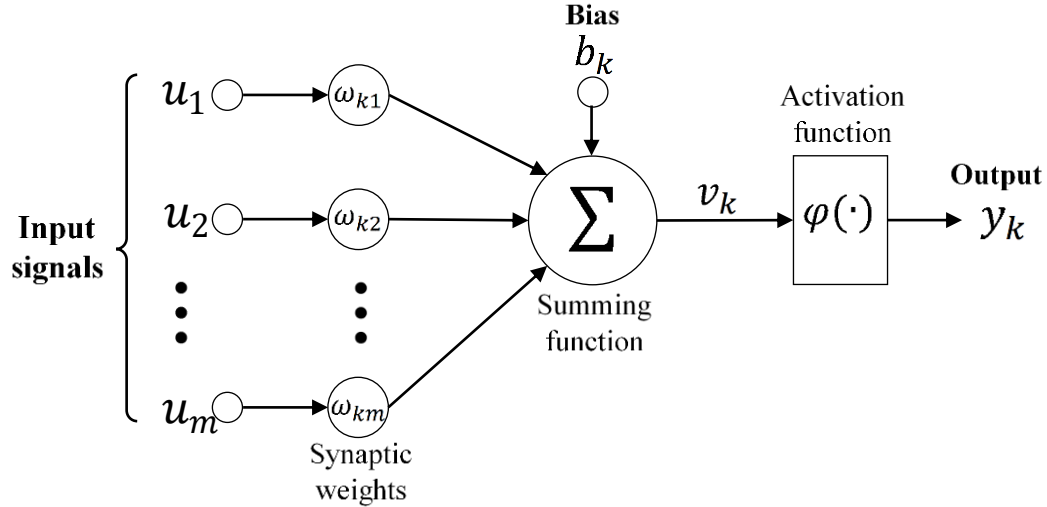


Figure 1.13: Graphical representation of an artificial neuron.

Mathematically the neuron can be described by:

$$y_k = \varphi \left(\sum_{j=1}^m u_j \omega_{kj} + b_k \right) \quad (1.3)$$

where, u_1, u_2, \dots, u_m are the input signals, b_k is the bias, $\omega_{k1}, \omega_{k2}, \dots, \omega_{km}$ are the synaptic weights of the neuron k , $\varphi(\cdot)$ is the activation function, v_k the action potential and y_k the neuron output.

•

1.5.1. Network architecture.

The ability of a neural network to learn depends in its architecture (Brett, 2015). Although there are countless forms of network architecture, they can be differentiated by three key characteristics:

- The number of layers.
- Whether information in the network is allowed to travel backward.
- The number of nodes within each layer of the network.

There are three main types of network architectures (Haykin, 2009):

i) *Single-layer feed forward.*

In this type of NN an input layer of source nodes is projected directly onto an output layer of neurons (**Figure 1.14**).

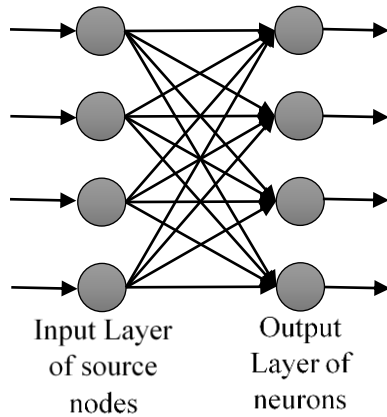


Figure 1.14: Single layer, fully connected neural network.

ii) *Multi-layer feedforward.*

Unlike the previous one, in this case there are at least three layers of neurons: the input layer, the output layer and an intermediate layer, also called the hidden layer. The term “hidden” refers to the fact that this part of the neural network is not seen directly from either the input or output of the network. In general, it is considered that one hidden layer should be sufficient for most problems, theoretically it has been shown that a neural network with a sufficiently large hidden layer can approximate any type of continuous function. However, a network with two hidden layers or more can solve some problems much more efficiently (Mas and Flores, 2008). The **Figure 1.15** shows a fully connected feedforward network with one hidden layer. The term fully connected indicate that each neuron receives the signals of all the neurons of the previous layer.

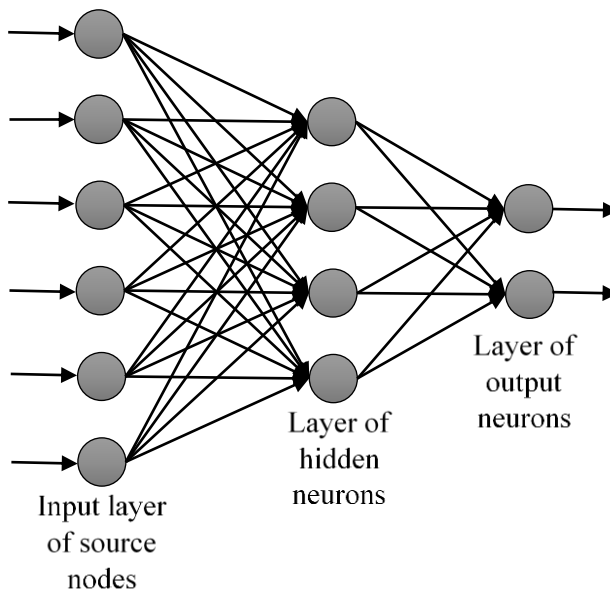


Figure 1.15: Fully connected feedforward network with one hidden layer and one output layer.

iii) *Recurrent Networks*

A recurrent neural network distinguishes itself from a feedforward neural network in that it has at least one feedback loop that requires the use of time delays (**Figure 1.16**). The presence of feedback loops has a profound impact on the learning capability of the network and on its performance.

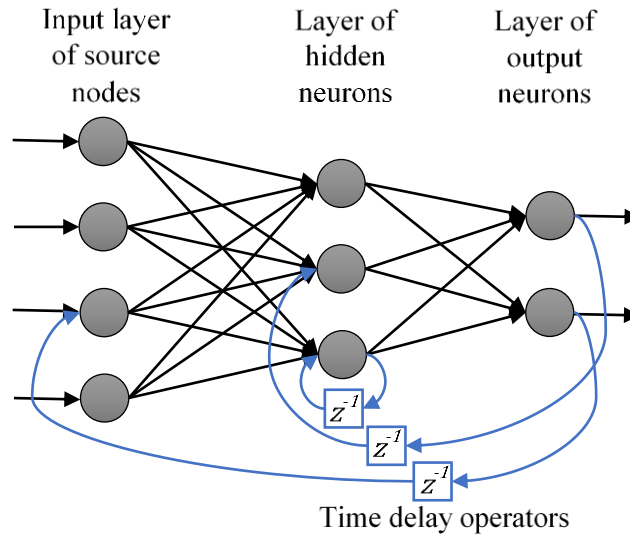


Figure 1.16: Recurrent network

1.5.2. Activation function.

The activation function $\phi(v)$ allows to establish the output of the neuron to which it is linked. The most used activation functions are (Brett, 2015):

i) Unit step activation function:

$$\varphi(v) = \begin{cases} 1, & \text{if } v \geq 0 \\ 0, & \text{if } v < 0 \end{cases} \quad (1.4)$$

ii) Piecewise linear function, with unitary amplification in the linear region:

$$\varphi(v) = \begin{cases} 1, & \text{if } v \geq +1/2 \\ v, & \text{if } +1/2 \geq v \geq -1/2 \\ 0, & \text{if } v \leq -1/2 \end{cases} \quad (1.5)$$

iii) Sigmoid activation function (Logistic sigmoid). The output explores all the values between 0 and 1. Here c us the slope parameter:

$$\varphi(v) = \frac{1}{1 + e^{-cv}} \quad (1.6)$$

- iv) Hyperbolic tangent function. It is a function like the logistic sigmoid and differs from it by being antisymmetric with values between -1 and 1:

$$\varphi(v) = \frac{1 - e^{-2cv}}{1 + e^{-2cv}} \quad (1.7)$$

1.5.3. Learning processes.

Learning processes can be classified into two categories: learning with a teacher and learning without a teacher. The **Figure 1.17** shows the block diagram of learning with teacher, in this process an input set is presented to the neural network, which processes the data and delivers an output that is compared with the real answer given by the teacher, the parameters of the network (weights and bias) are modified based on the calculated error (Gurney, 1997).

In the learning without a teacher the network modifies its parameters through previously defined rules.

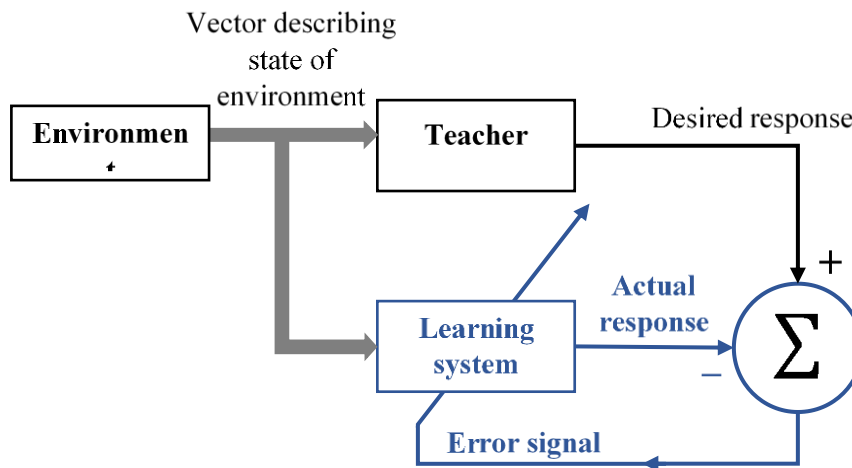


Figure 1.17: Block diagram of learning with a teacher, the part of the figure printed in blue constitutes a feedback loop.

Backpropagation Algorithm

Backpropagation (BP) algorithm is a widely used algorithm for training feedforward neural networks. The BP algorithm consist of two consecutives phases: feedforward, and backpropagation. In the first phase an input vector is presented to the network and propagated forward, to the output, then in the second phase, the network output is compared to the desired output, network weights and biases are then adjusted in accordance with an error-correction rule. A summary of all the steps involved in the training of an multilayer perceptron is presented above (Mas and Flores, 2008).

1. *Initialization.* Assign random numbers to synaptic weights, using a uniform random distribution
2. *Forward phase.* For each pair $(u(n), y(n))$ in the training set, its propagated the input signals through the net, layer by layer, as indicated in equation (1.8)

$$v_k^l(n) = \sum_{i=0}^{m_0} \omega_{ki}^l \hat{y}_i^{l-1}(n) \quad (1.8)$$

$$y_k^l = \varphi_k(v_k(n))$$

3. *Backpropagation phase.* The error signals corresponding to each neuron is computed.

$$e_k = y_k(n) - \hat{y}_k(n) \quad (1.9)$$

were $y_k(n)$ is the desired output of neuron k and $\hat{y}_k(n)$ is the actual output of neuron k . Then, its compute the local gradients of the network, defined by

$$\delta_k^l(n) = \begin{cases} e_k^{(L)}(n) \varphi_k(v_k^{(L)}(n)) \\ \varphi_k(v_k^{(L)}(n)) \sum_m \delta_m^{(l+1)}(n) \omega_{mk}^{(l+1)}(n) \end{cases} \quad (1.10)$$

Neuron k in output layer L
Neuron k in hidden layer l

where φ_k denotes differentiation with respect to the argument. Finally, the synaptic weights of layer l are adjusted following the generalized delta rule.

$$\omega_{ki}^l(n+1) = \omega_{ki}^l(n) + \alpha[\omega_{ki}^l(n-1)] + \eta \delta_k^l(n) \hat{y}_i^{l-1}(n) \quad (1.11)$$

where η is the learning rate that is used to update the internode weights, and α is the momentum constant. The momentum term uses the previous weight configuration to determine the direction of search for the global minimum of the error and allows the backpropagation algorithm to ‘pick up speed’ if a number of consecutive steps change the weights in the same direction (Mas and Flores, 2008).

The steps 2 and 3 are repeated for each example n in the training set and for each epoch, until the stop condition is met. The stop condition can be a given number of epochs, the error reaches a given value, or convergence seems to have stopped.

As an alternative to the BP algorithm, several training algorithms have been proposed. The Levenberg-Marquardt (LM) is a network training function that updates weight and bias values according to Levenberg-Marquardt optimization, it does not need learning rate and momentum so they can be easier to use than backpropagation.

1.5.4. Use NN for Real-time estimation for monitoring and control.

One of the most valuable features of neural networks is the possibility of real-time estimation of system variables, as opposed to delayed measurement using hardware measurement devices.

Any measuring instrument requires a finite time to perform the necessary actions to obtain the value of the final variable. This time varies depending on the type of measurement being carried out, for example if a chromatograph is used, the measurement time is of the order of minutes or even longer. In addition, if the measurement time is comparable with the dynamics of the system, delays that reduce the performance of the control system may occur (Fortuna *et al.*, 2007).

Auto-regressive models with exogenous inputs (ARX) or nonlinear ARX (NARX) allow making finite (and small) predictions of a variable. It is possible to use these models for real-time estimation of a system variable and replace measuring instruments with high measurement time (Zulkeflee and Aziz, 2009).

1.5.5. Nonlinear autoregressive exogenous model (NARX),

The nonlinear autoregressive exogenous model (NARX) relates the current value of a time series to both past values of the same series, and current and past values of the driving (exogenous) series (Billings, 2013). Mathematically can be written as:

$$y_t = F(y_{t-1}, y_{t-2}, y_{t-3}, \dots, u_t, u_{t-1}, u_{t-2}, \dots) + \varepsilon_t$$

Here \mathbf{y} is the variable of interest, and \mathbf{u} is the externally determined variable. In this scheme, the actual and old values of \mathbf{u} , together with past values of \mathbf{y} itself, helps to predict \mathbf{y}_t . Here ε is the error term (sometimes called noise), and the function F is some nonlinear function such as a polynomial. F can be a neural network, a wavelet network, a sigmoid network and so on.

There are two different architectures of NARX model: series-parallel architecture (named also open-loop), and parallel architecture (named also close-loop). The mathematical description is given by the equations (1.12) and (1.13), respectively

$$\hat{y}(t+1) = F(y(t), y(t-1), \dots, y(t-n_y), u(t+1), u(t), u(t-1), \dots, u(t-n_x)) \quad (1.12)$$

$$\hat{y}(t+1) = F(\hat{y}(t), \hat{y}(t-1), \dots, \hat{y}(t-n_y), u(t+1), u(t), u(t-1), \dots, u(t-n_x)) \quad (1.13)$$

In the case of Neural-Network-based NARX model, F is the mapping function of the neural network, $\hat{y}(t+1)$ is the output of the NARX at the time $t+1$ (it is the predicted value of y), $\hat{y}(t)$, $\hat{y}(t-1)$, ..., are the past outputs of the NARX. $y(t)$, $y(t-1)$, ..., are the true past values of the times series, called also desired outputs values. These situations are illustrated in **Figure 1.18**.

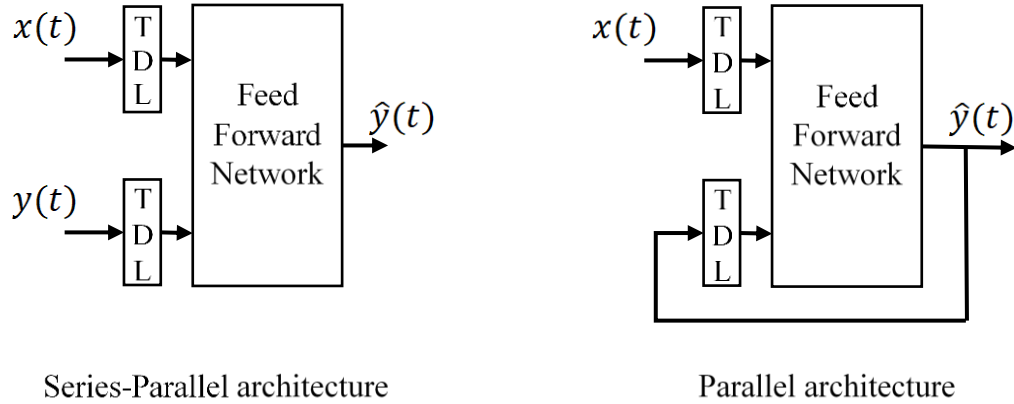


Figure 1.18: Architectures of the NARX neural network

In the open-loop architecture the future value of the time series is predicted from the present and past value of $u(t)$ and the past values of the time series $y(t)$. On the other hand, in the close loop architecture the prediction is made based on the present value and the past of $u(t)$ and the past values predicted by the neural network $\hat{y}(t)$.

The mapping function $F(\cdot)$ is initially unknown and it is approximated during the training process of the prediction. In the NARX neural network model, the internal architecture that performs this approximation is the Multi-Layer Perceptron (MLP). The MLP offers a powerful structure allow to learn any type of continuous nonlinear mapping (Boussaada *et al.*, 2018).

The objective of this work is the development of a soft sensor based on neural networks for the prediction of vapor concentration inside a methanol tank equipped with an inerting system. Knowing the vapor concentrations inside the tank allows to identify hazardous situations and always ensure the safe operation of the system, monitoring with physical sensors is not always possible due to economic limitations and technical challenges, and prediction with dynamic models requires in-depth knowledge of the system. A neural network is proposed to be used for concentration prediction. Neural networks are computational models that allow modeling of systems without prior information because they have the ability to learn by training with examples, plus, due to their parallel connections they allow high information transmission rates and almost immediate response, which makes them the perfect candidates to operate in real time. In addition, they have an easy implementation and coupling with existing technology.

To achieve this goal, first the mathematical model of the tank was developed starting from phenomenological principles and making some considerations to facilitate its implementation in Matlab. Once the behavior of the system at different inputs was verified, the response surface of the system flammability conditions to random variations of different amplitudes in the input variables was evaluated. Next, four soft sensor configurations based in neural network models are proposed and trained and tested with two different data sets obtained through the mathematical model. Each configuration is tested and the one with the best performance is selected. Finally, the chosen soft sensor is tested further to evaluate its performance in a situation where flammable

conditions are reached inside the tank. It was found that the best performing soft sensor configuration is configuration B, which has the most input variables, this configuration can satisfactorily predict concentrations in the tank even when the system enters flammable conditions. The creation, training and testing of the networks was done through the deep-learning tool of Matlab.

2. Materials and methods.

2.1. Description of the storage tank

A vertical storage tank with a fixed roof and a capacity of 100 m³ is here considered as a case study. It is designed to store the methanol required for a process, allowing a constant flow, and always guaranteeing the availability of the reagent. **Figure 2.1** shows the tank design with the main inlet and outlet lines.

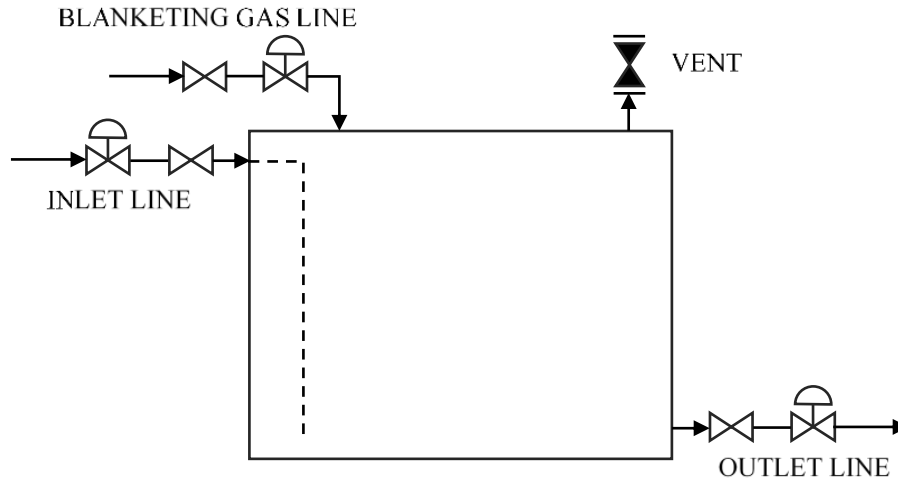


Figure 2.1: Methanol storage tank.

The tank geometry is cylindrical, has a flat roof and operates at atmospheric pressure. Its dimensions are 6.6 m in height and 4.4 m in diameter. The main components of the tank are:

- **Inlet line:** allows the filling of the tank, it consists of a pipe located at the upper part of the tank and is extended to a few centimeters before the bottom of the tank.
- **Outlet line:** allows the extraction of the substance through a pump, it is located at the bottom of the tank.
- **Blanketing gas line:** Provides the nitrogen that helps to avoid the formation of an explosive atmosphere inside the tank.
- **Vent:** Mechanical device designed to provide pressure or vacuum release.

As mentioned above, the purpose of the tank is to provide a constant supply of methanol. On the one hand, the methanol is extracted through the outlet line and fed to the process through a system of pipes and pumps, it is supposed that the methanol outflow is equal to 245.1 kg h⁻¹. On the other hand, when the liquid level is less than 30% of the tank's total capacity, the filling phase proceeds, and methanol is fed at a rate of 41178.8 kg h⁻¹ until the tank level reaches 80%. The feeding rate was calculated assuming that this is done with 26 m³ tanker trucks that take approximately 30 minutes to unload all its contents.

Due to the restrictions and the hazards of methanol storage, the system has a nitrogen line that helps to compensate the pressure drop due to the emptying and prevents the concentration of oxygen from reaching flammable levels. In normal operation the nitrogen flow remains constant and is equal to 0.1753 kg h^{-1} . This flow was obtained through the model implemented in Matlab and is the one that guarantees a constant oxygen concentration equal to 8%.

The vent valve allows to maintain the pressure close to the atmospheric value allowing vapors to escape from the headspace or air to enter depending on whether the system is pressurized or at vacuum. The evaluated tank has a 102 mm diameter vent valve which is configured to let vapors out when the system overpressure is greater than 7 kPa and let air in when the vacuum pressure is greater than 1 kPa. The setpoint values of the vent valve were established according to the criteria for methanol storage tank proposed by Bechtold (1997).

The oxygen concentration set point for this tank is defined as two percentage points below the LOC as recommended by CEN (2006). That is, the oxygen concentration to be maintained inside the tank is equal to 8%.

The **Table 2.1:** Methanol tank dimensions and operative conditions summarizes the main tank characteristics and operating conditions.

Table 2.1: Methanol tank dimensions and operative conditions

Shell Height	6.6	m
Shell Diameter	4.4	m
Maximum Liquid Height	5.3	m
Total volume	100.4	m^3
Working Pressure	101325	kPa
Working Volume	80.3	m^3
Temperature	293	K
Breather vent vacuum setting	1	kPa
Breather Vent Pressure setting	7	kPa
Minimum flow area vent	5	cm^2
Outflow of methanol	245.11	kg h^{-1}
Inflow of Nitrogen	0.175	kg h^{-1}
Methanol mole fraction setpoint	8%	

The independent variables of the system are the methanol output and the nitrogen input. During plant operation the methanol outflow and nitrogen inflow may vary from their stationary values due to operational changes.

2.2. *Mathematical model of the storage tank*

For the mathematical model, the tank is divided into two subsystems: the liquid phase and the gas phase. Only liquid methanol is present in the liquid phase, while the gas phase is constituted by a mixture of nitrogen, oxygen, and methanol. With the aim of facilitating the calculations we consider the vent as two separate streams, F_4 and F_5 . The first is the air input flow due to the

vacuum pressure condition of the system, while the second is the vapor mixture output flow due to the overpressure. The **Figure 2.2** shows the sketch of the system.

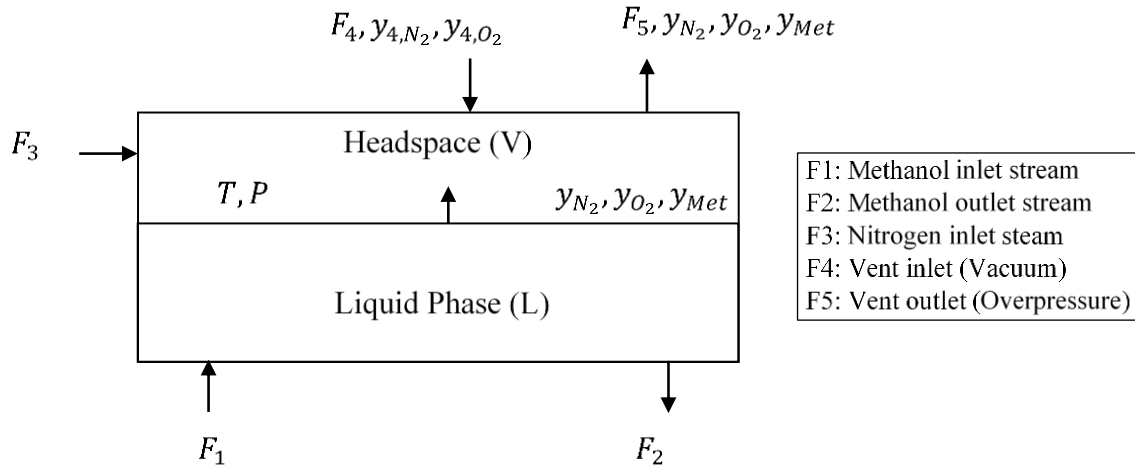


Figure 2.2: Flow diagram for the methanol tank

For the development of the model, it is assumed that the temperature outside the tank remains constant and the temperature changes inside the tank due to methanol evaporation are small, so changes in liquid volume and pressure due to temperature are not taken into consideration. It is also assumed that the liquid is incompressible and does not react with the gas phase. Finally, the gas phase is considered as a well-mixed system that obeys the ideal gas law and the transfer of material takes place only from the liquid phase to the gas phase, i.e., there is no dissolution of oxygen and nitrogen in the liquid and no condensation of methanol.

The **Table 2.2** shows all the variables involved in the system with their respective nomenclature and the corresponding units in the international system

Table 2.2: List of variables and nomenclature.

Nomenclature	Variable	Units SI
F_1	Inlet stream of pure liquid methanol	[kg s ⁻¹]
F_2	Outlet stream of pure liquid methanol	[kg s ⁻¹]
F_3	Inlet stream of pure gas nitrogen	[kg s ⁻¹]
F_4	Inlet stream of air	[kg s ⁻¹]
F_5	Outlet stream of vapors	[kg s ⁻¹]
N^L	Total number of moles in liquid phase	[kmol]
N^V	Total number of moles in vapor phase	[kmol]
N_1	Total molar flow to vessel stream 1	[kmol s ⁻¹]
N_2	Total molar flow to vessel stream 2	[kmol s ⁻¹]
N_3	Total molar flow to vessel stream 3	[kmol s ⁻¹]
N_4	Total molar flow to vessel stream 4	[kmol s ⁻¹]
N_5	Total molar flow to vessel stream 5	[kmol s ⁻¹]
A	Cross sectional area	[m ²]
\emptyset	Molar flux of methanol from liquid to vapor	[kmol m ⁻² s ⁻¹]
N_{Nit}^V	Number of moles of nitrogen in vapor phase	[kmol]
N_{Oxy}^V	Number of moles of oxygen in vapor phase	[kmol]
N_{Met}^V	Number of moles of methanol in vapor phase	[kmol]
$y_{4,Oxy}$	Mole fraction of oxygen in air	
$y_{4,Nit}$	Mole fraction of nitrogen in air	
y_{Nit}	Mole fraction of nitrogen in vapor phase	
y_{Oxy}	Mole fraction of oxygen in vapor phase	
y_{Met}	Mole fraction of methanol in vapor phase	
k_{Met}^V	mass transfer coefficient for methanol	[kmol m ⁻² s ⁻¹]
y_{Met}^*	saturation mole fraction of methanol	
P_{Met}^*	saturation pressure of methanol	[Pa]
P	pressure of the vessel	[Pa]
V_{tot}	vessel volume	[m ³]
V^L	volume of liquid phase	[m ³]
V^V	volume of vapor phase	[m ³]
ρ	liquid density	[kg m ⁻³]
MW_{Met}	molecular weight of methanol	[kg kmol ⁻¹]
MW_{av}	average molecular weight of vapor phase	[kg kmol ⁻¹]
MW_{Nit}	molecular weight of nitrogen	[kg kmol ⁻¹]
MW_{Oxy}	molecular weight of oxygen	[kg kmol ⁻¹]
MW_{Air}	molecular weight of air	[kg kmol ⁻¹]
R	universal gas constant	[J kmol ⁻¹ K ⁻¹]
T	temperature of the system	[K]

The mass balances for the methanol storage tank are presented below.

Species balance for each species in the liquid phase (only methanol):

$$\frac{dN^L}{dt} = N_1 - N_2 - A * \phi \quad (2.1)$$

Species balance for each species in the gas phase:

$$\frac{dN_{Nit}^V}{dt} = N_3 + N_4 y_{4,Nit} - N_5 y_{Nit} \quad (2.2)$$

$$\frac{dN_{Oxy}^V}{dt} = N_4 y_{4,Oxy} - N_5 y_{Oxy} \quad (2.3)$$

$$\frac{dN_{Met}^V}{dt} = A \phi - N_5 y_{Met} \quad (2.4)$$

Interphase mass transfer relation:

$$\phi = k_{Met}^V (y_{Met}^* - y_{Met}) \quad (2.5)$$

Equilibrium at phase boundary:

$$y_{Met}^* = \frac{P_{Met}^*}{P} \quad (2.6)$$

Molar holdup of gas phase:

$$N_{Nit}^V = N^V y_{Nit} \quad (2.7)$$

$$N_{Met}^V = N^V y_{Met} \quad (2.8)$$

$$N_{Oxy}^V = N^V y_{Oxy} \quad (2.9)$$

Volume constraint:

$$V_{tot} = V^L + V^V \quad (2.10)$$

Summation of mole fractions:

$$y_{Met} + y_{Nit} + y_{Oxy} = 1 \quad (2.11)$$

Volume/Mass relationship:

$$V^L = N^L MW_{Met} \frac{1}{\rho} \quad (2.12)$$

Average molecular weight gas phase:

$$MW_{av} = y_{Met} MW_{Met} + y_{Nit} MW_{Nit} + y_{Oxy} MW_{Oxy} \quad (2.13)$$

Mol/Mass relationship:

$$N_1 = \frac{F_1}{MW_{Met}} \quad (2.14)$$

$$N_2 = \frac{F_2}{MW_{Met}} \quad (2.15)$$

$$N_3 = \frac{F_3}{MW_{Nit}} \quad (2.16)$$

$$N_4 = \frac{F_4}{MW_{Air}} \quad (2.17)$$

$$N_5 = \frac{F_5}{MW_{av}} \quad (2.18)$$

Ideal gas law:

$$P V^V = N^V R T \quad (2.19)$$

To know if the system under study is well specified, the degrees of freedom analysis is used. The total number of variables/quantities listed in the **Table 2.2** is 37, of which 13 are invariant parameters of the system (**Table 2.3**), while only 2 variables (F1, F2) are independent variables. The total number of equations written for the system is equal to 19.

Table 2.3: Invariant parameters.

1	A
2	$y_{4,Oxy}$
3	$y_{4,Nit}$
4	K_{Met}^V
5	P_{Met}^*
6	V_{tot}
7	MW_{Met}
8	MW_{Nit}
9	MW_{Oxy}
10	MW_{Air}
11	R
12	T
13	ρ

From the analysis of the degrees of freedom (**Table 2.4**) it is obtained that the system is underspecified, making necessary the search for additional relationships that allow the solution of the system of equations. In addition to the equations presented above, the relationship between the level and the Input methanol flow is known, and the equation (2.20) is used for the estimation of the flow through the vent (F_4 and F_5). This provides two additional equations and one additional relationship between the variables.

Table 2.4: DOF Analysis

37	<i>Number of quantities</i>
-13	<i>Time invariant parameters</i>
-2	<i>Independent variables</i>
-19	<i>Number of equations</i>
3	<i>DOF</i>

Gas Flows through the vents

The equation (2.20) is used to calculate the flow through the vent valve. This equation gives the theoretical flow through the air vents (American Petroleum Institution, 1998):

$$F'_{vent} = 12503P_{1,v}A_v \sqrt{\frac{k}{W_{air}TZ(k-1)} \left[\left(\frac{P_{2,v}}{P_{1,v}}\right)^{\frac{2}{k}} - \left(\frac{P_{2,v}}{P_{1,v}}\right)^{\frac{k+1}{k}} \right]} \quad (2.20)$$

where,

F'_{vent}	= Theoretical flow rate, in normal cubic meters per hour	$[\text{Nm}^3 \text{h}^{-1}]$
A_v	= Minimum flow area of device	$[\text{cm}^2]$
$P_{1,v}$	= Pressure at device inlet	$[\text{bar}]$

$P_{2,v}$	= Pressure at device outlet	[bar]
k	= Ratio of specific heats of test medium (For Air $k \approx 1.4$)	
W_{air}	= Molecular weight of air	[kg kmol ⁻¹]
T	= Absolute temperature at the device inlet	[K]
Z	= Compressibility factor, evaluated at inlet conditions (if unknown, use $Z = 1$).	

2.2.1. Calculation of time invariant parameters.

Mass transfer coefficient for methanol

The mass transfer coefficient can be estimated using the relationship (Crowl and Louvar, 2011):

$$K = aD^{\frac{2}{3}} \quad (2.21)$$

where, a is a constant and D is the gas phase diffusion coefficient. This equation is used to determine the ratio of the mass transfer coefficients between the species of interest K and a reference species K_0 :

$$\frac{K}{K_0} = \left(\frac{D}{D_0}\right)^{2/3} \quad (2.22)$$

The gas phase diffusion coefficients are estimated from the molecular weights of the species:

$$\frac{D}{D_0} = \sqrt{\frac{MW_0}{MW}} \quad (2.23)$$

Combining the equations gives:

$$K = K_0 \left(\frac{MW_0}{MW}\right)^{\frac{1}{3}} \quad (2.24)$$

Water is most frequently used as a reference substance; it has a mass transfer coefficient of 0.83cm/s.

Saturation pressure

The vapor pressure is calculated using the Antoine Equation:

$$\log_{10}(P) = A - \left(\frac{B}{T + C}\right) \quad (2.25)$$

where P is the vapor pressure in bar and T is the temperature of the gas in K. The parameters were taken from the NIST and are reported on the **Table 2.5**.

Table 2.5: Antoine Equation parameters. Data from NIST.

Temperature (K)	A	B	C	Reference
353.5 - 512.63	5.15853	1569.613	-34.846	Ambrose, Sprake, et al., 1975
288.1 - 356.83	5.20409	1581.341	-33.50	Ambrose and Sprake, 1970
353. - 483.	5.31301	1676.569	-21.728	Hirata and Suda, 1967

Liquid Density

To calculate the density of the methanol the Equation (2.26) is used:

$$\rho_L = A \cdot B^{-\left(1-\frac{T}{T_c}\right)^n} \quad (2.26)$$

where A , B , T_c , and n , are parameters reported in the literature, T in K and ρ in g ml^{-1} . For methanol in the range of $175\text{K} < T < 512.6 \text{ K}$ see **Table 2.6**.

Table 2.6: Density Equation parameters. Data from (Coker, 2010).

A	B	n	T_c	Range
0.27197	0.27192	0.23310	512.58	$175\text{K} < T < 512.6 \text{ K}$

2.3. Soft Sensor design.

The purpose of the soft sensor is to predict the concentration in the headspace of the tank. It is assumed that in the gaseous part there are three substances present: Nitrogen, Oxygen and Methanol. It is defined that the output of the sensor will be the mole fractions of nitrogen and methanol, while the oxygen concentration is calculated through the unity sum of the fractions.

As possible input variables are the following independent variables: methanol outlet, and nitrogen inlet; in addition, the methanol inlet and the level measurement are supposed to be available. Since there is no access to the physical tank, the data set is generated using the mathematical model described earlier and is not filtered because it was obtained with the subrogated model and the presence of outliers is considered improbable.

An autoregressive neural network with exogenous inputs was selected as the model structure since it is recommended for the prediction of time series data in nonlinear systems. A set of 4 different layouts was used, to determine which presents the best performance in the studied case.

2.3.1. Layout A

In this layout the input variables to the soft sensor are the methanol inlet and outlet flows as well as the nitrogen flow. These variables are fed to two independent neural networks, which calculate the nitrogen and methanol fraction respectively.

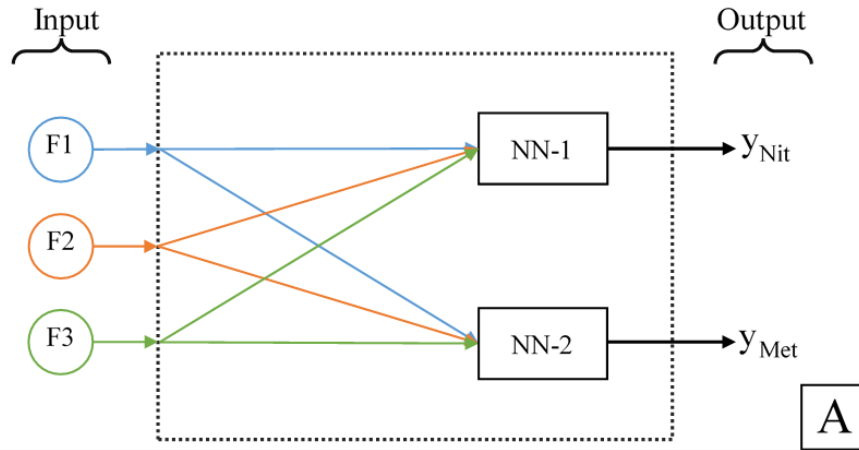


Figure 2.3: Soft sensor Layout A.

2.3.2. Layout B

This arrangement is similar to the previous one, but this one take advantage of the availability of the level measurement as additional variable. All the inputs are fed to two independent neural networks that calculate the nitrogen and methanol fractions.

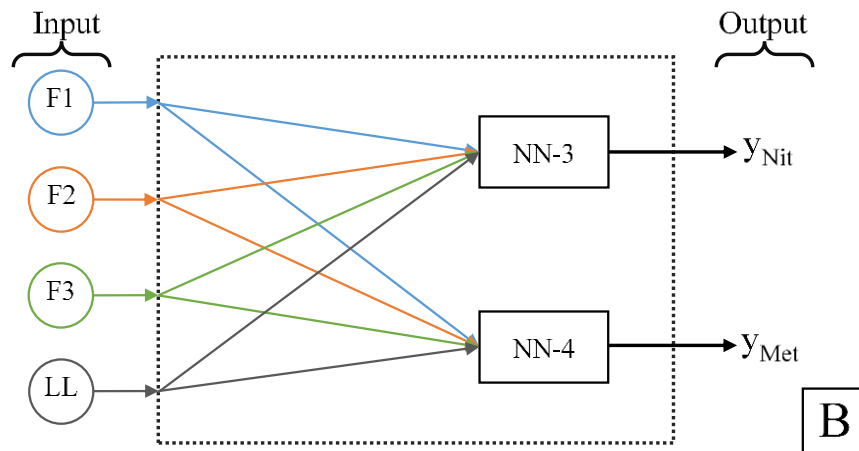


Figure 2.4: Soft sensor Layout B.

2.3.3. Layout C

The input variables of the soft sensor are F1, F2 and F3, these variables are fed to a first neural network (NN-5) that predicts the level inside the tank. This value is then fed, together with the input values, to two neural networks identical to those used by layout B.

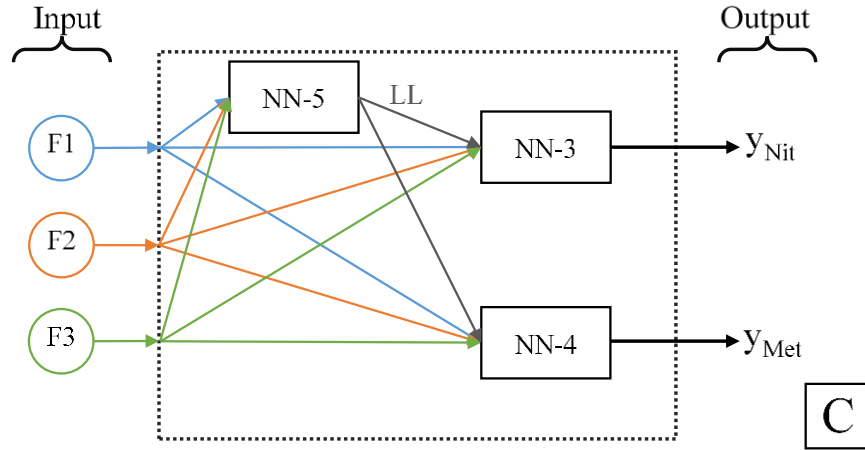


Figure 2.5: Soft sensor Layout C.

2.3.4. Layout D

The objective of this layout is to see if it is possible to reduce the number of sensors required by the system to two: for this purpose the level and the nitrogen inflow were selected as inputs. The level is selected as input because it is strongly dependent on the inflow and outflow of the reservoir. The NN-6 and NN-7 neural networks are used to predict the nitrogen and methanol fractions respectively.

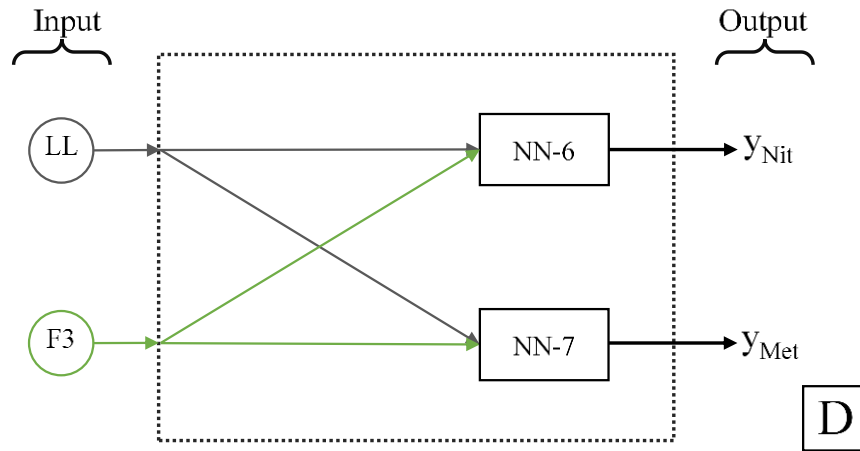


Figure 2.6: Soft sensor Layout D.

2.4. Neural networks description.

The networks used for the soft sensors were implemented in Matlab® using its Neural Time Series Tool and using the Nonlinear autoregressive with External (Exogenous) Input (NARX) model, which is useful to predict series $y(t)$ given d past values of $y(t)$ and another series $x(t)$.

The **Figure 2.7** shows the procedure followed for the creation and training of the neural network. The first step is to load the learning data set, which is constituted by a time series of input-output pairs, then the architecture of the network is defined by defining the inputs and outputs of

the network with their respective delay. Also, the number of layers, the transfer functions for each layer and the number of neurons must be indicated.

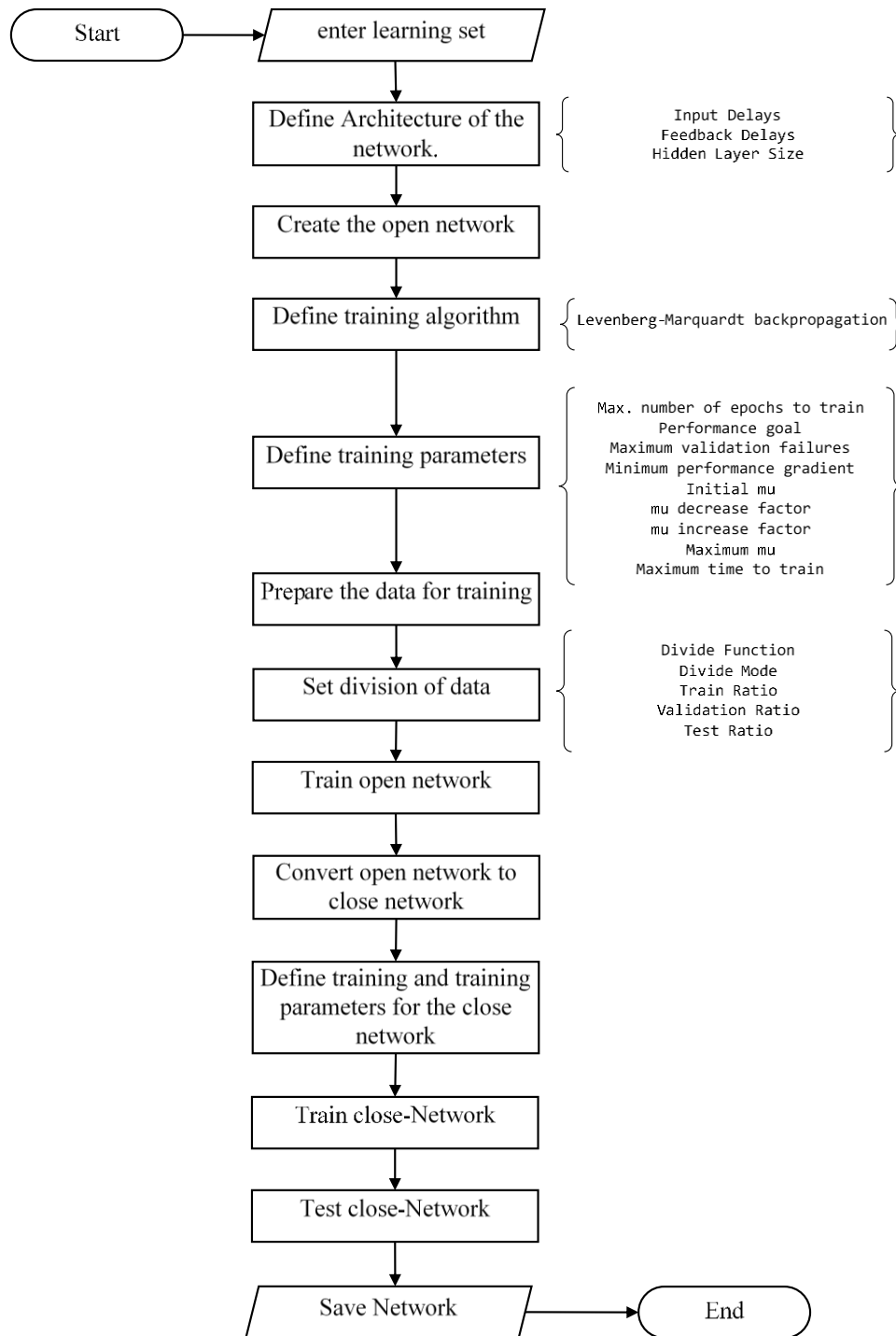


Figure 2.7: Procedure followed for the creation and training of the neural network.

The procedure starts from an open-loop neural network that is trained to initialize the network parameters (weights and biases), once obtained the trained open-loop-network, its transform into a close-loop-network and trained again with the same learning set. To guarantee the non-overfitting we tested the network with a data set different to those using in the learning stage. The performance of the test is checked and finally the neural network is saved. The Matlab code used for the creation and training of the NARX Neural Network is presented in Appendix A: Matlab code - Creation and training NARX Neural network..

The **Table 2.7** shows the input parameters for the neural networks used.

Table 2.7: Neural networks used in the soft sensor.

	NN-1	NN-2	NN-3	NN-4	NN-5	NN-6	NN-7
Input	F1, F2, F3	F1, F2, F3	F1, F2, F3, LL	F1, F2, F3, LL	F1, F2, F3	LL, F3	LL, F3
Output	Y_{Nit}	Y_{Met}	Y_{Nit}	Y_{Met}	LL	Y_{Nit}	Y_{Met}
Number of layers	1	1	1	1	1	1	1
Number of neurons	15	15	29	29	12	25	10
Input delay	2	2	3	3	1	4	2
Feedback delay	2	2	3	3	2	3	2
Training Function	trainlm	trainlm	trainlm	trainlm	trainlm	trainlm	trainlm

2.5. Dataset generation.

The neural network learning and testing data sets consist of a set of input-output variable pairs. Usually, the datasets are generated from the historical information of the process stored in the data center of the industries. in this case, since there is no access to the physical measurements of the tank, it is decided to use the mathematical model to generate these datasets.

To generate the datasets, a procedure consisting of three steps is followed: first, a matrix is generated with values of the independent variables over time; then, this matrix is fed to the mathematical model where a matrix with the values of all the process variables is obtained; and finally, with all the available data the input-output pairs are assembled according to the neural network to be trained, for example, for NN-1 the dataset is composed of pairs $\{[F1, F2, F3]-[Y_{Nit}]\}$.

The evaluation of the response of the system to changes in the input variables is done by generating a vector of independent values that varies randomly over time and then is following the same procedure described above.

2.6. Input random generation.

To generate the random input, it is first defined the sampling time, the periodicity of the variation of the variable, the steady state values of the system and the range of variation of the

variables. The periodicity of variation corresponds to the time it takes for the variable to change its value to a new one. Then, using the random generator function, a random value of the input within the defined range of amplitude is generated. Then, using the spline function, a smooth curve is made by joining all the random points and sampling each sampling time. Finally, a rescaling of the data is performed to ensure that the amplitude limits of the variation are respected. The Matlab code used for the creation the input random sequence is presented in Appendix B: Matlab code - Input Random Generation

The sampling time was defined based on the time taken for the tank to be filled from 30% to 80% of its capacity. In the present case study, with the established conditions, the filling time is around 1 h, so one-sixth of the filling time, i.e. 10 min, is selected as the sampling time. On the other hand, for the periodicity of variation, 90 is chosen, which means that the input variable takes 15 h to go from one value to another.

The **Figure 2.8** shows an example of the input random generation for a variable with steady state value of 1, range of variation of $\pm 70\%$ and a periodicity of variation equal to 10. In the first subplot, the random variables are generated, then with using the spline function and the sampling time a smooth curve is obtained, lastly, the rescale of the values guarantee that the limits are not exceeded.

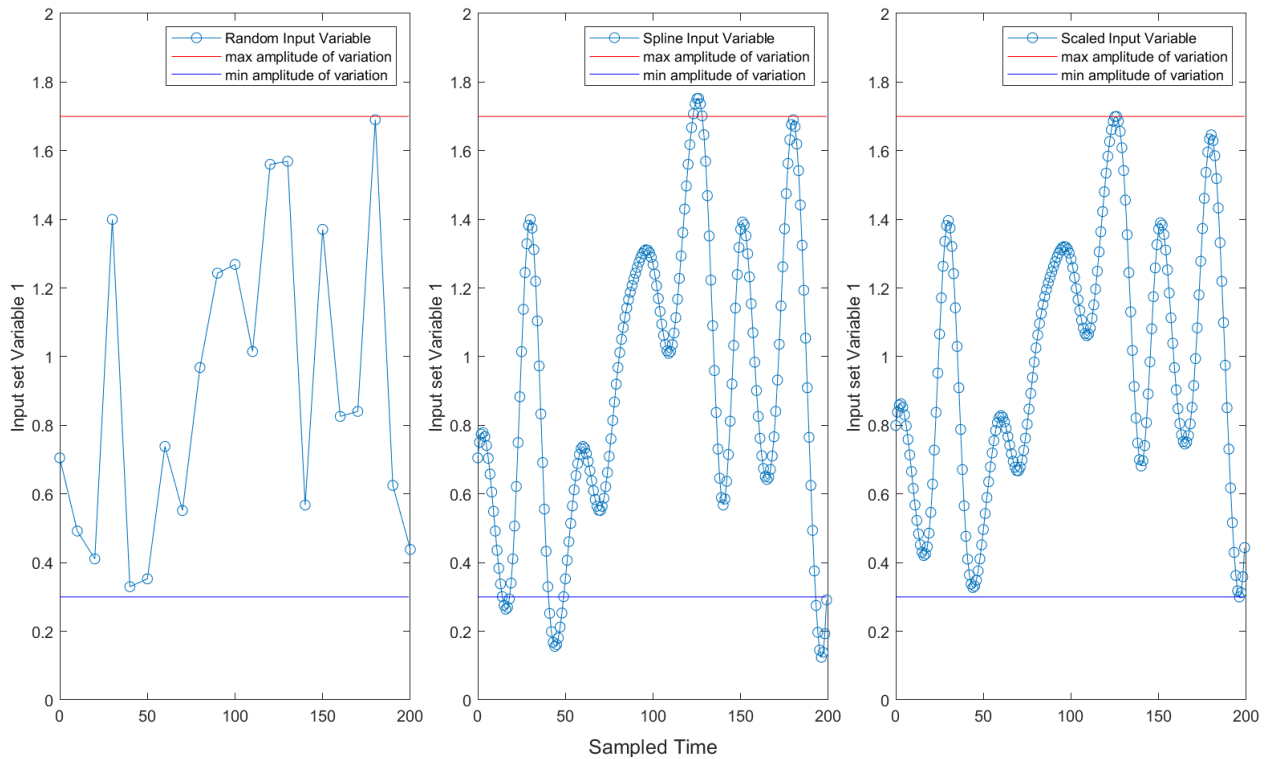


Figure 2.8: Random vector generation example.

2.7. Procedure followed

The **Figure 2.9** shows the procedure followed to obtain the soft sensor. First, the mathematical model of the tank was generated using the equations described in section 2.1. To solve the system of differential equations, the ODE23 solver incorporated in Matlab was used. Since there is no experimental data to validate the mathematical model, only a verification that the model works properly and responds as expected is made, for this purpose the model is fed with step type pulses in the input variables (F2 and F3), the response of the system is observed in order to confirm the expected behavior and the relationship between the variables.

The response in the flammability coordinates of the system to a random input of defined maximum amplitude is studied. The ranges of variation for F2 and F3 were 20%, 40%, 60% and 80% for each of them. The algorithm described in section 2.6. was used to generate a data set with an extension of 300,000 points for each variation of the input amplitude. A total of 8 datasets were generated, one for each variation range. Then, each one of the data sets is presented to the mathematical model that gives the value of all the variables of the system at each moment. With the concentrations in the headspace, the flammability coordinates are calculated and the results are plotted. The objective of this test is to determine the minimum range of variation for each variable that could generate a risk situation in the system.

The range of F2 and F3 in which the system explores conditions close to the flammability peninsula are selected. Subsequently a new input dataset of 45,000 points with a simultaneous random variation of F2 and F3 is created, this input is fed to the mathematical model and all the values of the system variables are stored, this large amount of data is the database from which the data required for the training of the neural networks is taken. The test data is obtained in an analogous way by changing the ranges of variation and the length of the data set.

The neural networks were created and trained using the algorithm presented in the section 2.4. the pairs input-output were selected according with the network to train and the values were taken from the database created previously. Subsequently, the performance of all the neural networks is evaluated using the same test data. The best layout was chosen based on two criteria: the mean square error and the graphical comparison between the predicted and expected response.

At last, the layout with the best performance is selected as proposed soft sensor and is further tested to evaluate the behavior of the virtual sensor in a situation where the system enters in flammable conditions.

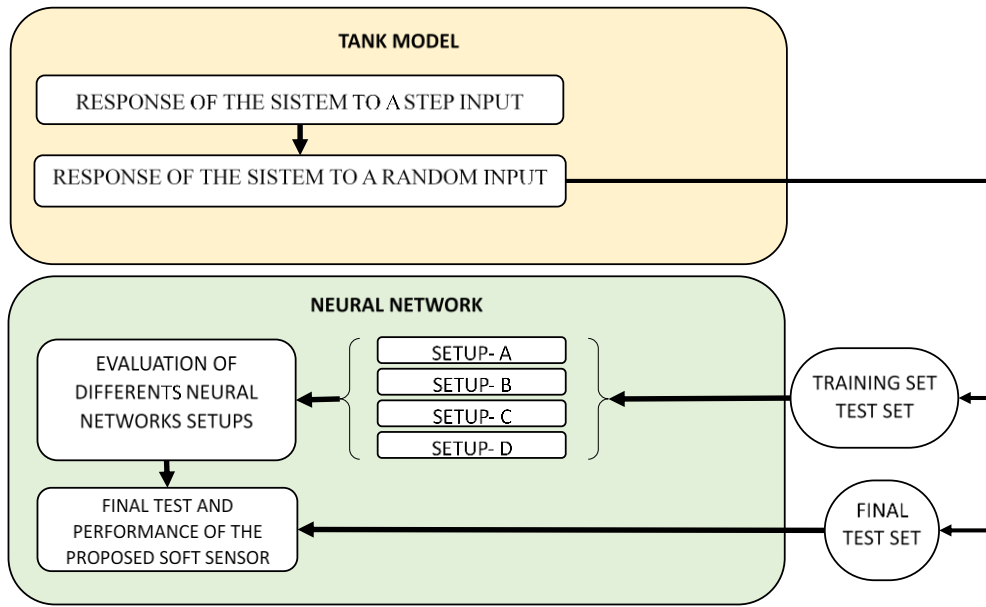


Figure 2.9: Procedure followed for the development of the soft sensor.

3. Results and discussion.

3.1. Response of the system to a step function.

The behavior of the system to a step variation in the inputs is evaluated **Figure 3.1** and **Figure 3.2** show the response of the system when a step in the methanol outflow (F2) is applied, keeping constant the value of the nitrogen flow (F3). When F2 is increased by 30% of its stationary value (**Figure 3.1**) an increase in the oxygen concentration and a decrease in the nitrogen concentration is observed, while the methanol concentration remains approximately constant. **Figure 3.2** shows the response when the F2 value is decreased, in this case the methanol fraction remains constant, while nitrogen fraction increase and oxygen fraction decrease.

Figure 3.3 and **Figure 3.4** report the response of the system when F3 is varied keeping F2 constant. In both figures It can be observed that the oxygen concentration varies inversely with the change in F3, i.e., it decreases as the value of F3 increases. While the nitrogen concentration varies directly with F3.

In all the scenarios evaluated, it is observed that after the filling process is completed, the nitrogen concentration increases but the methanol and oxygen concentrations decrease temporarily. This can be explained because when filling the volume available for the vapors decreases generating an increase in the pressure, if its higher than the setpoint of the vent the gases are allowed to escape. At the end of the filling step the quantity of gases is reduced, and the tank is slightly pressurized, as the nitrogen flow and methanol output are keeping constants the increasing in the nitrogen concentration occurs. As time goes on, the pressure recovers and the variation in the concentrations present a similar behavior to the one observed before filling.

The concentration inside the tank depends on the values of F2 and F3 in that F3 must be set to recover the pressure lost when the tank is emptied. When the value of F3 is not able to maintain the pressure, a vacuum situation is generated and air is allowed to enter, resulting in an increase in oxygen concentration. On the other hand, when the opposite situation occurs, i.e., when there is a higher F3 flow than required to balance the pressure drop, an overpressure situation appears and vapors are allowed to escape, with a consequent decrease in oxygen content. The methanol fraction remains approximately constant because it depends mainly on the methanol saturation pressure.

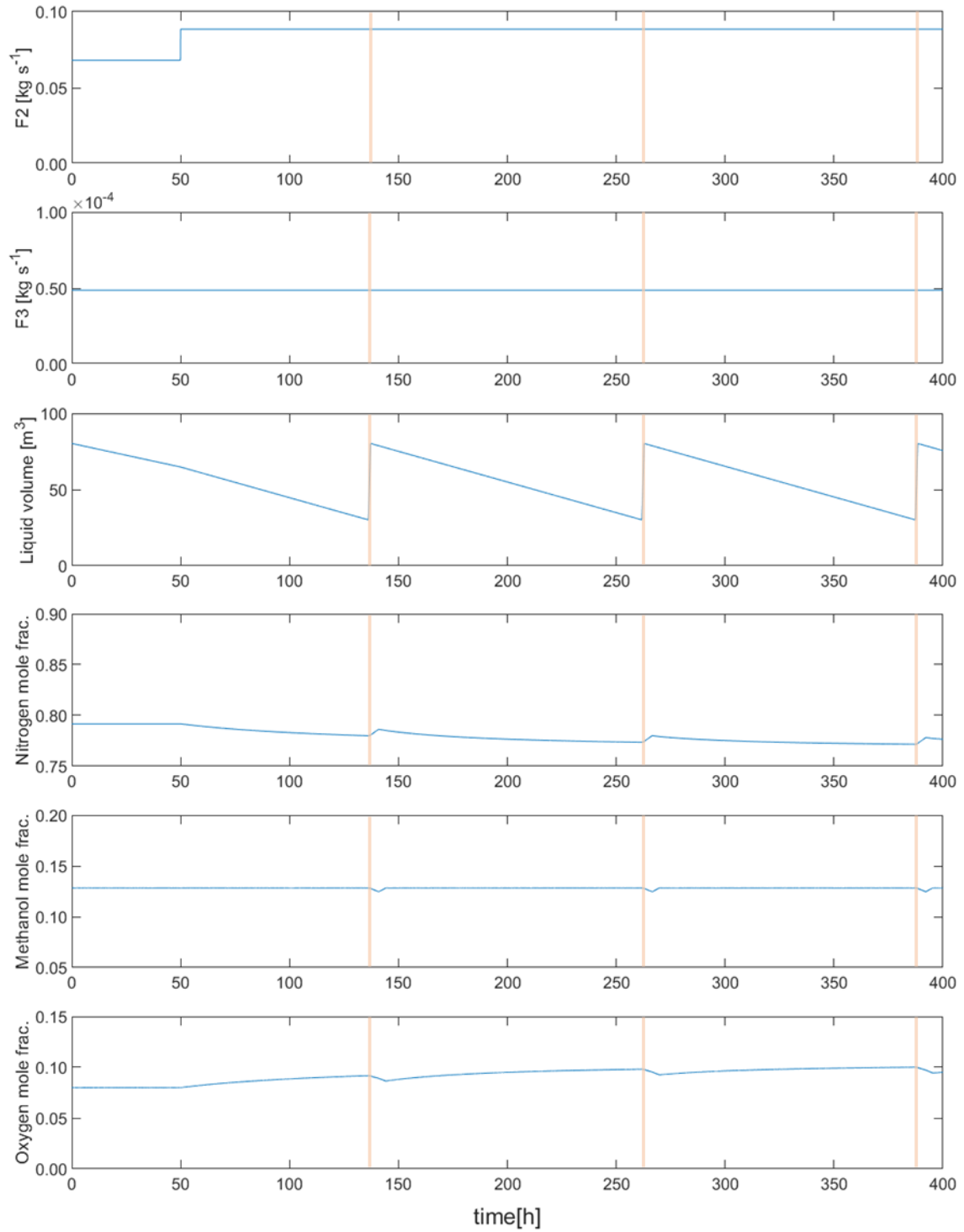


Figure 3.1: Response of the tank when a step in F2 equal to +30% of the steady state value at time = 50 h is applied. The orange vertical bar is used to indicate the filling time of the tank.

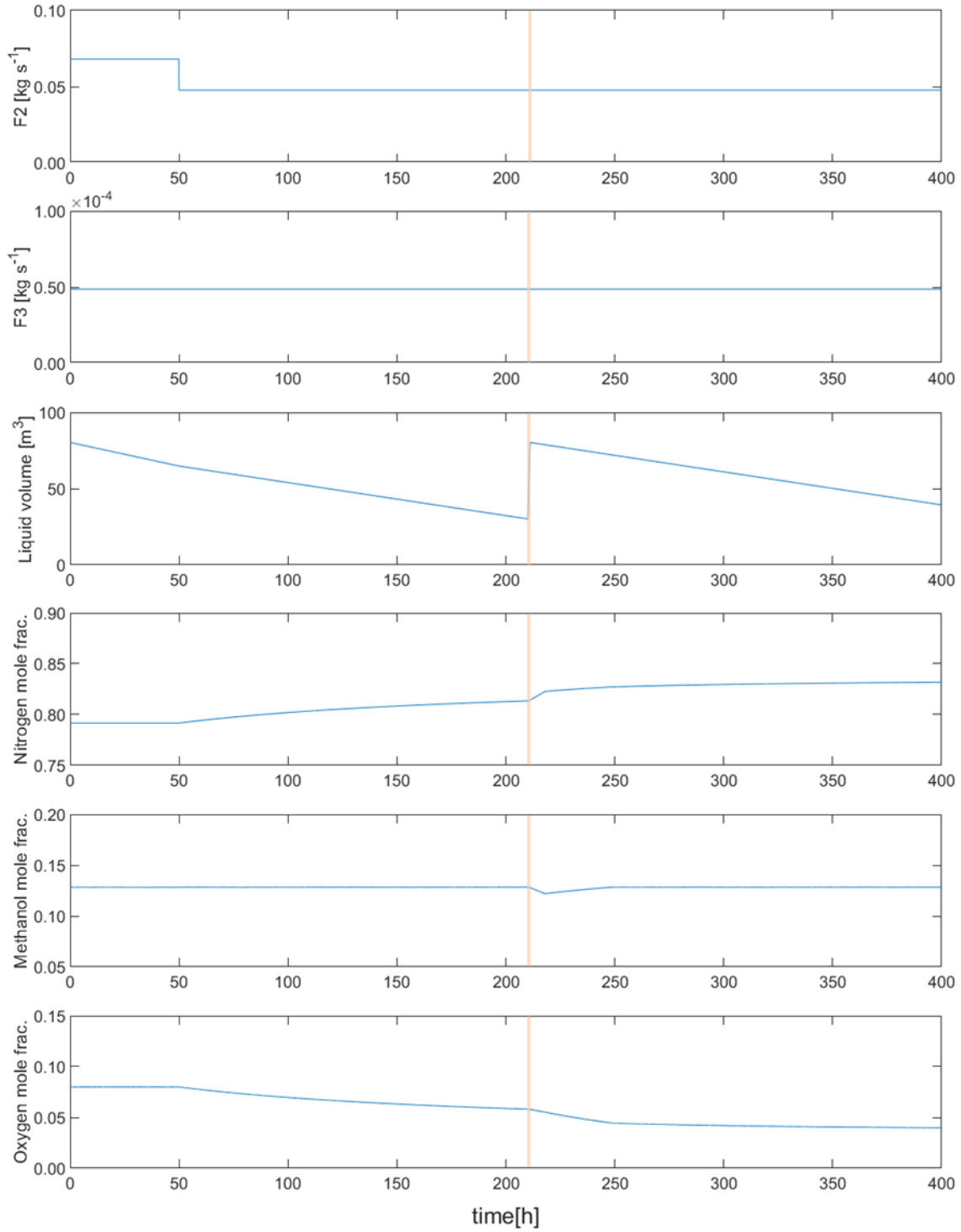


Figure 3.2: Response of the tank when a step in F2 equal to -30% of the steady state value at time = 50h is applied. The orange vertical bar is used to indicate the filling time of the tank.

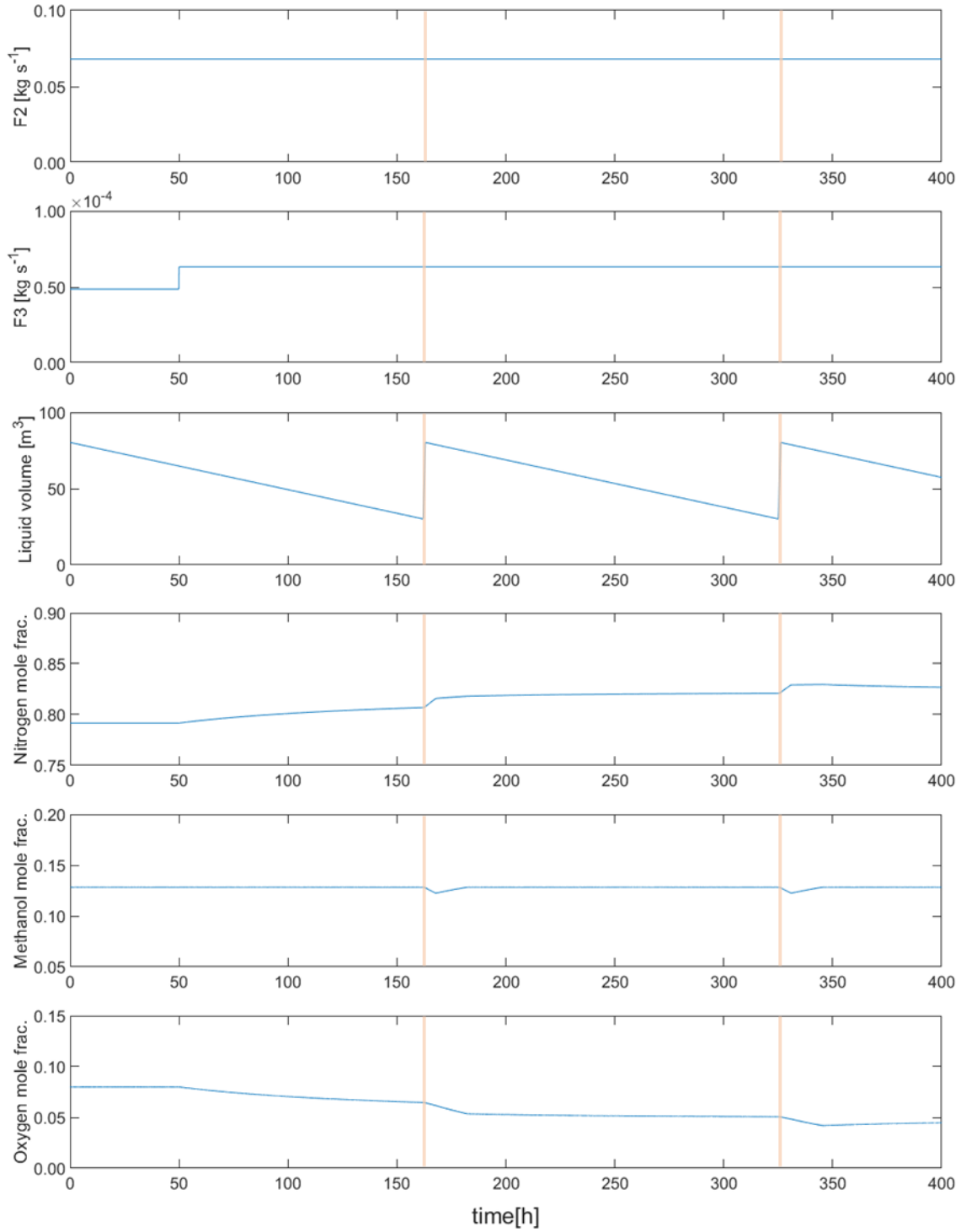


Figure 3.3: Response of the tank when a step in F3 equal to +30% of the steady state value at time = 50 h is applied. The orange vertical bar is used to indicate the filling time of the tank.

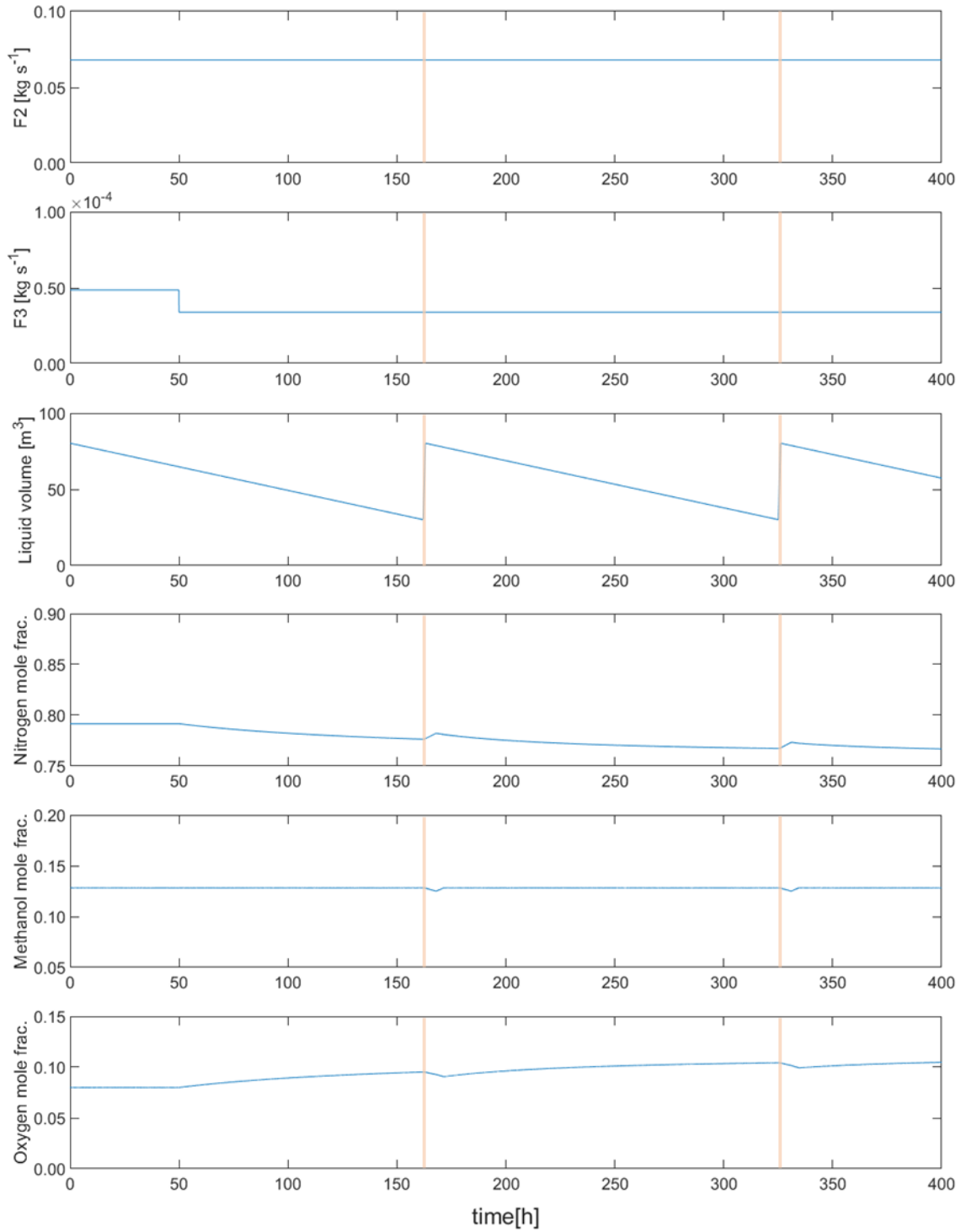


Figure 3.4: Response of the tank when a step in F3 equal to -30% of the steady state value at time = 50 h is applied. The orange vertical bar is used to indicate the filling time of the tank.

3.2. Response of the system to a random input.

The flammability conditions inside the tank were evaluated when the variables F2 and F3 are randomly varied over time within the ranges: 20%, 40%, 60% and 80%. **Figure 3.5** shows the response surface obtained by varying F2; as expected, as the range of variation increases, the response surface increases; for the first three evaluated cases A, B and C the flammability conditions are not reached with the used data set. Also, it is observed that the system reaches the flammability conditions (enters the peninsula) only when the variation of F2 is in the range of 80%.

Figure 3.6 shows the results when F3 is varied, it is observed that the response surfaces of the system are similar in size and shape to those obtained in **Figure 3.5**, which suggests that changes in F2 and F3 produce responses of similar magnitude in the system.

The study of the system response is taken as a basis for defining the ranges of variation of the learning set used for the training of the neural networks, a range of variation equal to 80% for F2 and F3 is selected, and the tank is simulated for 7500 h. The system response to the input of the learning dataset used is shown in **Figure 3.7**. It is observed that by combining the effect of the two variables the response surface of the system is increased, in this case it enters more deeply into the flammability peninsula.

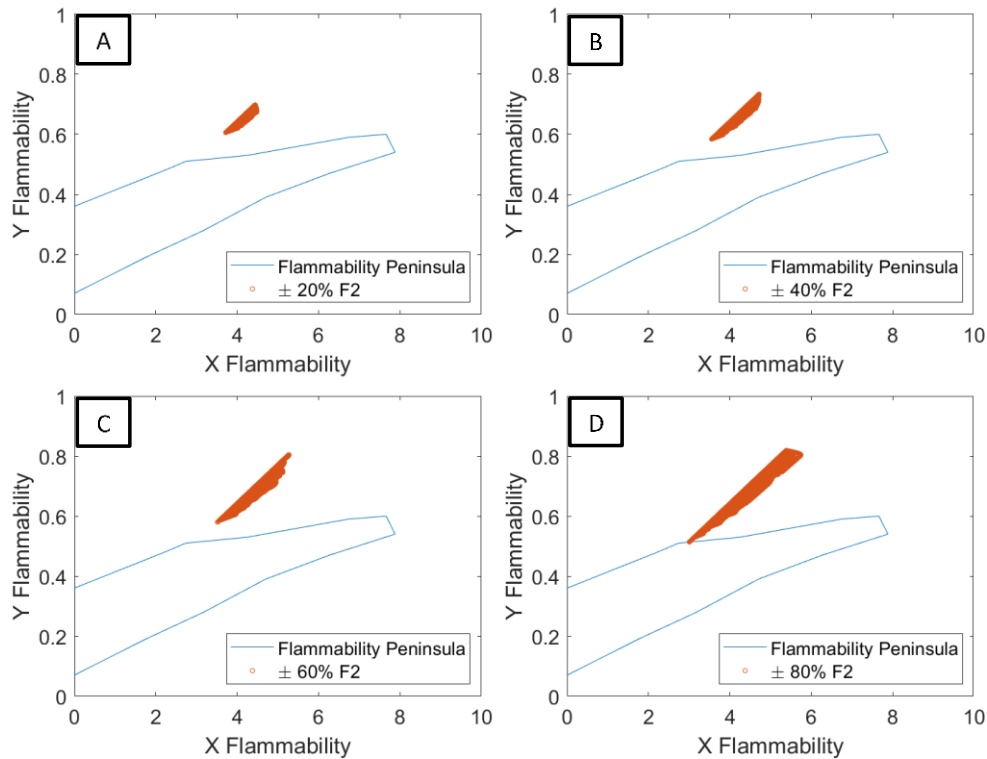


Figure 3.5: Variation of flammability conditions inside the tank for a random input in time of F2 keeping F3 constant.

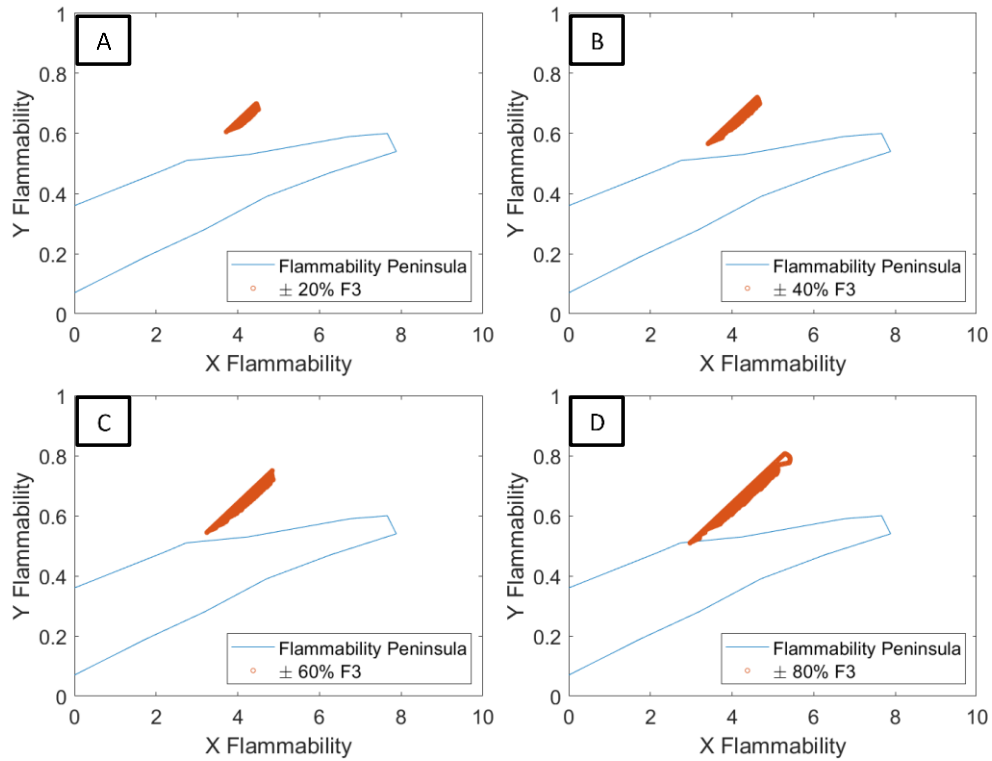


Figure 3.6: Variation of flammability conditions inside the tank for a random input in time of F3 keeping F2 constant.

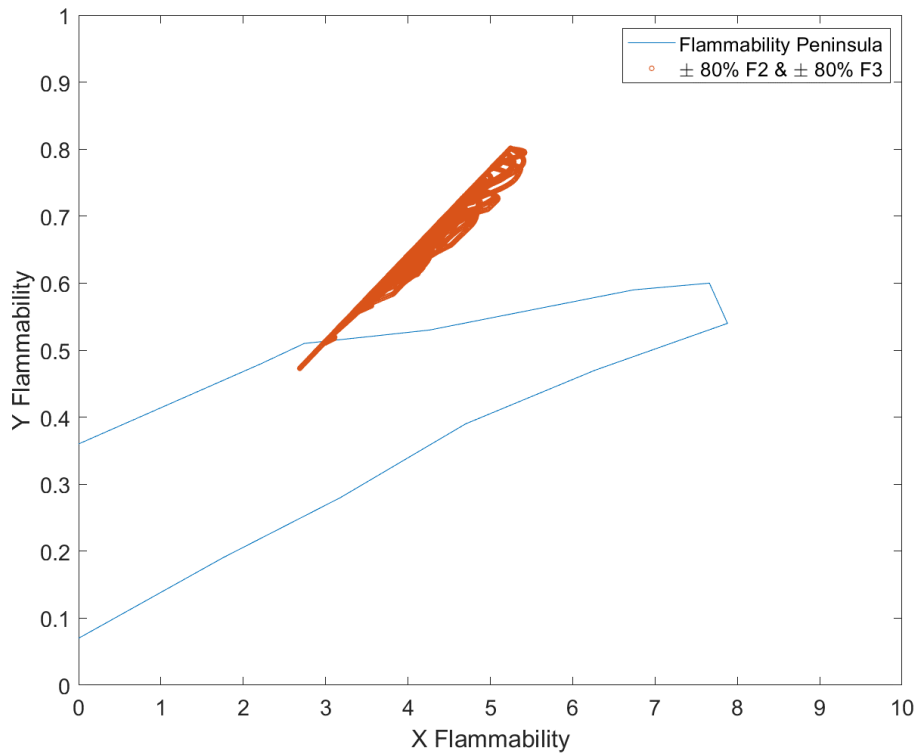


Figure 3.7: Flammability diagram for the learning set using in the network training.

3.3. Evaluation of different soft sensor setups.

The **Table 3.1** presents the mean squared error (MSE) for the prediction obtained with the trained neural networks when the data set used for learning is presented.

Table 3.1: MSE calculated for the prediction of the trained neural networks for the learning set.

	SETUP-A	SETUP-B	SETUP-C	SETUP-D
MSE y_{Met} prediction	1.2E-07	4.6E-09	1.5E-06	1.1E-06
MSE y_{Nit} prediction	5.0E-06	2.9E-07	5.4E-07	3.4E-05

The best MSE was obtained with setup B which has F1, F2, F3 and LL as input, while the neural network with the highest error was D which has LL and F3. This indicates that the presence of additional inputs has a positive effect on network performance.

To ensure that the overtraining phenomenon is not present and to evaluate the prediction of the system dynamics, an additional test is performed with all the trained networks. The **Figure 3.8** shows the data set employed for the test, this was obtained following the same procedure used to obtain the training set but changing the parameters of the random generation algorithm (section 2.6), setting the length of the data set equal to 6000 points and defining the range of variation for F2 and F3 at 50%. The sampling time was kept unchanged (10 min).

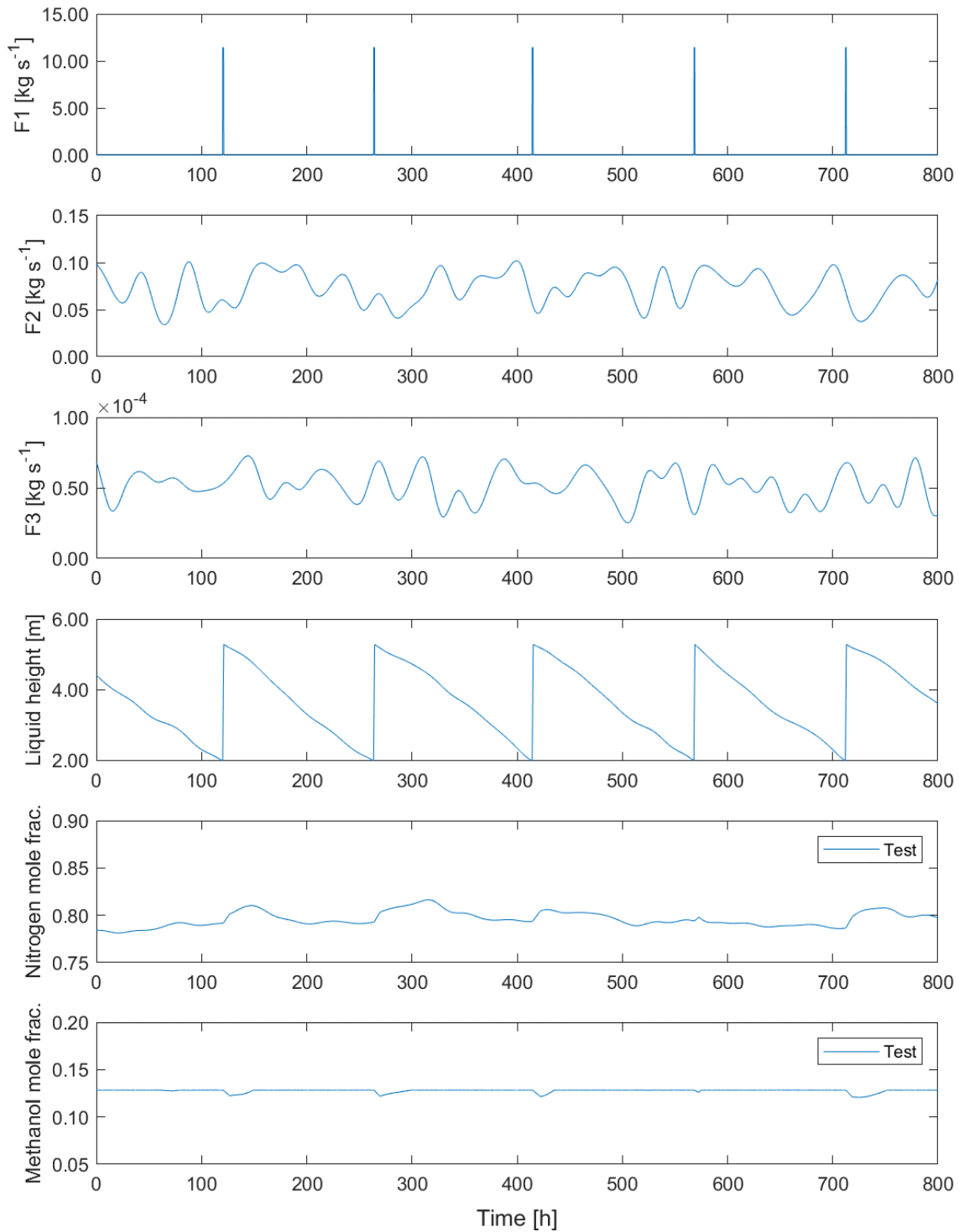


Figure 3.8: Data set for overtraining evaluation.

Figure 3.9 shows the comparison between the methanol concentration predicted by layout A and the target value, the vertical orange lines indicate the times at which the tank is filled. In the figure the residual of the error is higher around the filling time, however, in general terms it can be seen that the soft sensor is able to approximately predict the behavior of the methanol concentration.

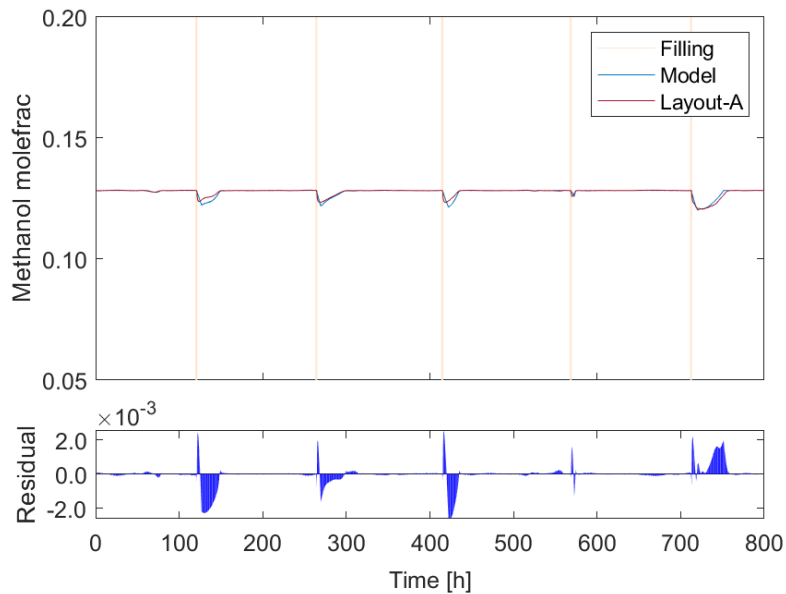


Figure 3.9: Concentration of methanol predicted by setup A.

The prediction of the nitrogen fraction when the input test is presented is shown in **Figure 3.10**. In this case, residues with a larger magnitude than in the case of methanol are presented, however, they present a larger distribution. The highest magnitude of the observed residue is equal to $10E-3$ and it is presented around the simulation time 150 h. As in the previous case, it is observed that the neural network is capable of capturing the generalities of the system behavior.

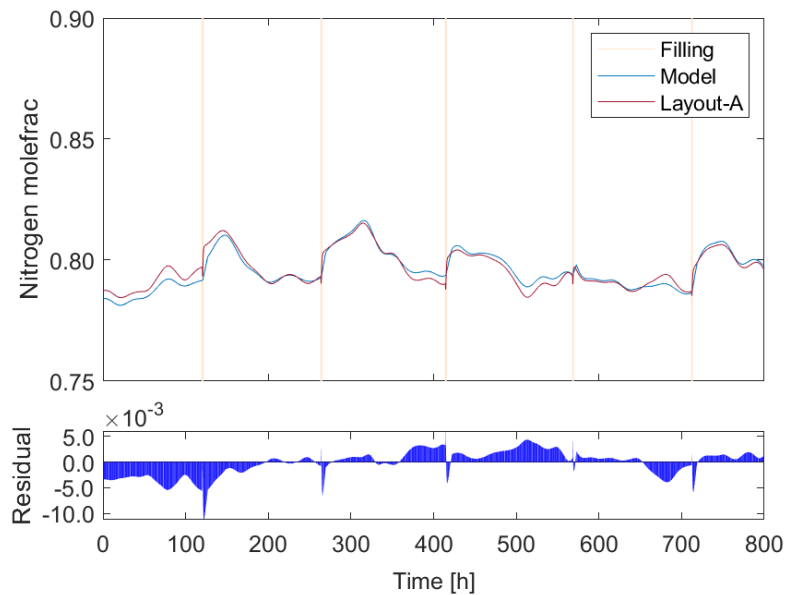


Figure 3.10: Concentration of Nitrogen predicted by setup A

Figure 3.11 shows the prediction of the methanol concentration obtained with layout B, which shows a better curve fit than that observed with layout A, in addition, the magnitude of the largest residual error obtained is equal to 1.0×10^{-3} .

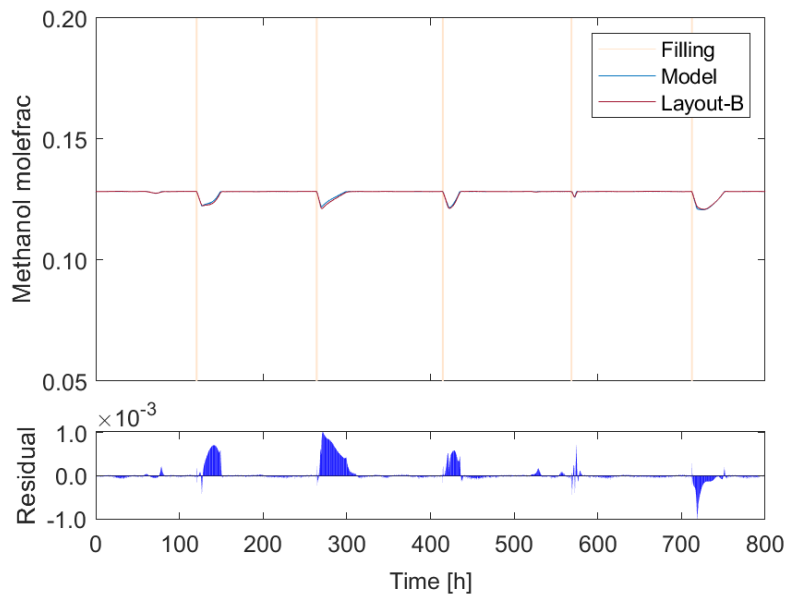


Figure 3.11: Concentration of Methanol predicted by setup B

In the **Figure 3.12** it is possible to observe that the nitrogen concentration line predicted by layout B is almost coincident with that of the target value, this is confirmed by the residuals, which are close to zero during the test, except in the areas close to the tank filling.

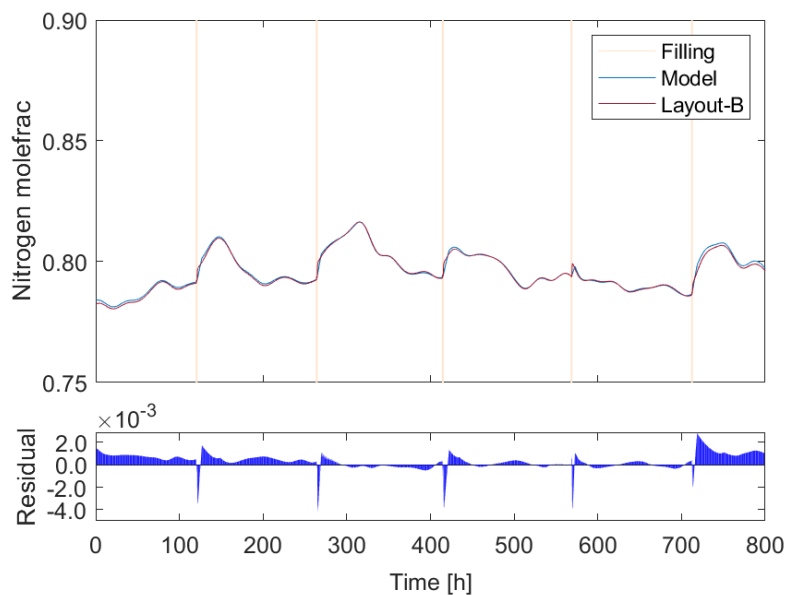


Figure 3.12: Concentration of Nitrogen predicted by setup B.

The prediction of the methanol fraction obtained with layout C follows a strange behavior in the hours immediately after the filling process (**Figure 3.13**), in the evaluated case the system reaches a maximum residual of approximately $20E-3$, while for layout A and B the maximum residuals were approximately $2E-3$ and $1E-3$ respectively.

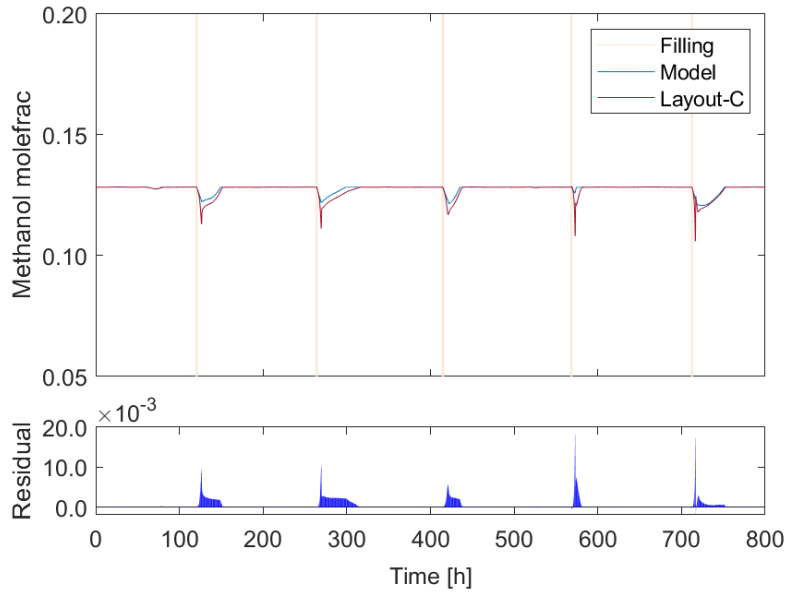


Figure 3.13: Concentration of Methanol predicted by setup C.

Figure 3.14 shows the prediction of the nitrogen concentration when setup C is used, showing a better coupling between the predicted value and the target. However, the calculated residuals are higher than those obtained with setup B.

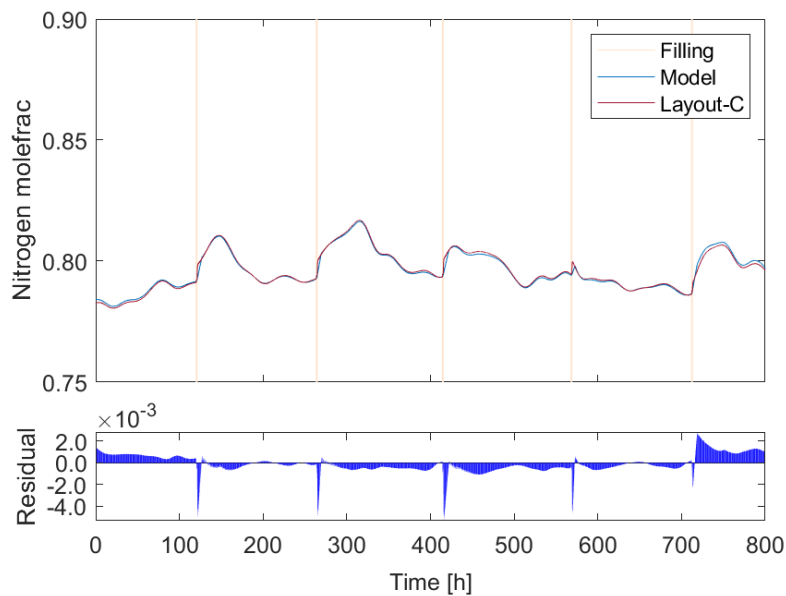


Figure 3.14: Concentration of Nitrogen predicted by setup C.

Layout D presents a poor representation of the behavior of methanol concentration, mainly when it shows a decrease. (Figure 3.15).

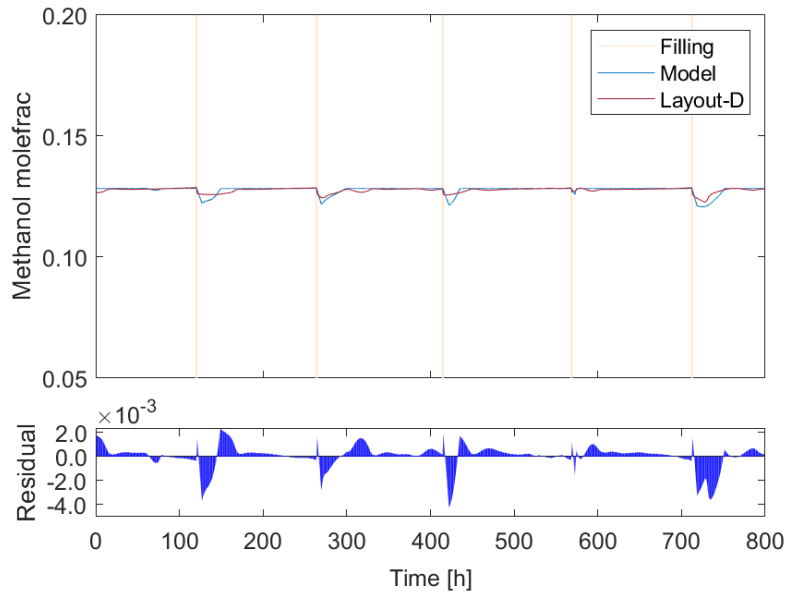


Figure 3.15: Concentration of Methanol predicted by setup D.

Figure 3.16 shows the comparison between the output of layout D and the target. In this case the soft sensor is not able to adequately predict the nitrogen concentration, moreover, the prediction line obtained shows a behavior completely different from the expected one, the residual plot indicates that in some points the magnitude of the difference between the predicted value and the expected value is greater than 0.02.

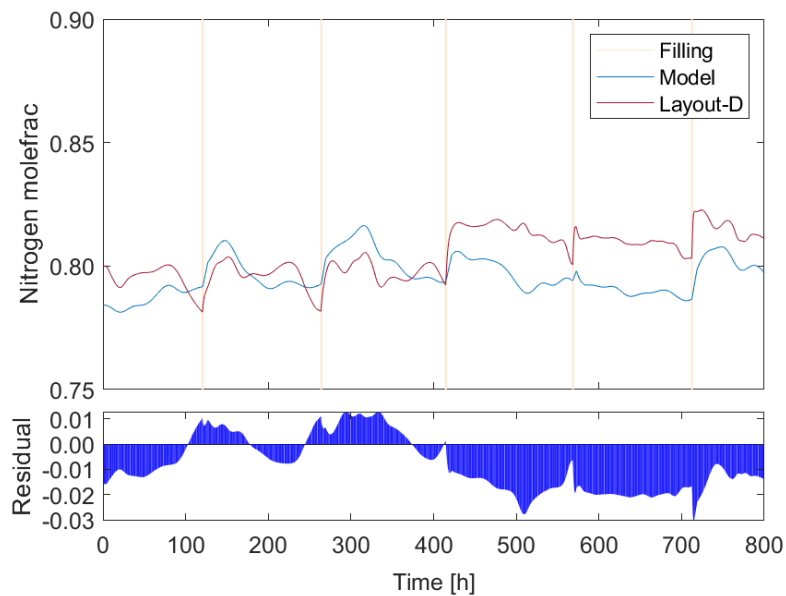


Figure 3.16: Concentration of Nitrogen predicted by setup D.

In addition to the graphical analysis presented above, **Table 3.2** shows the summary of the mean square error for each setup when the test data set was used. Compared to **Table 3.1**, it can be seen that the errors calculated for the test set are of the order of magnitude, or close, to the error obtained with the learning set, indicating that the training of the neural network has been done properly and that no overtraining is present.

Table 3.2: Performance of the neural network's configurations evaluated when test is presented.

	SETUP-A	SETUP-B	SETUP-C	SETUP-D
MSE y_{Met} prediction	2.4502e-07	3.2991e-08	1.8116e-06	8.2038e-07
MSE y_{Nit} prediction	9.5963e-06	7.5037e-07	8.4823e-07	1.7221e-04

It is observed that in all the evaluated cases, the system presents the highest residues in the zones close to the filling of the tank (orange vertical line), a possible reason to explain this is that it is in this zone where the greatest changes in the concentration of the system occur.

When the results obtained with setup A and setup B are compared, it is concluded that the presence of additional information about the level helps to improve the performance of the network, this is proven both by the graphical analysis and by the MSE results obtained. However, in setup C, which uses the same inputs as setup A (F1, F2, F3) and internally predicts the level in the tank, a decrease in the performance for the prediction of the concentrations is observed when compared to that obtained with setup B, which may indicate that the neural network used for the prediction of the level presents errors in its output that are amplified in the prediction of the methanol fraction.

For the final validation Setup B is selected based on the observed graphical response (**Figure 1.11 & Figure 1.12**) and on the MSE value obtained for the learning set and the test set.

3.4. Final test performance.

Setup B is selected to perform the final test and check its performance predicting the concentrations when the system enters into flammable conditions. **Figure 3.17** shows the results obtained, the blue box shows the input values fed to the soft sensor, while the orange one shows the comparison between the value obtained with the phenomenological model and the value predicted by the neural network. For the conditions evaluated the soft sensor can satisfactorily predict the concentrations.

Figure 3.18 shows the time variation of the oxygen fraction predicted by the mathematical model and compares it with the value calculated from predictions of methanol and nitrogen concentrations shown in **Figure 3.17**. As expected in this case also the system predicts satisfactorily the oxygen concentration, being able to predict even when the system is in flammable conditions.

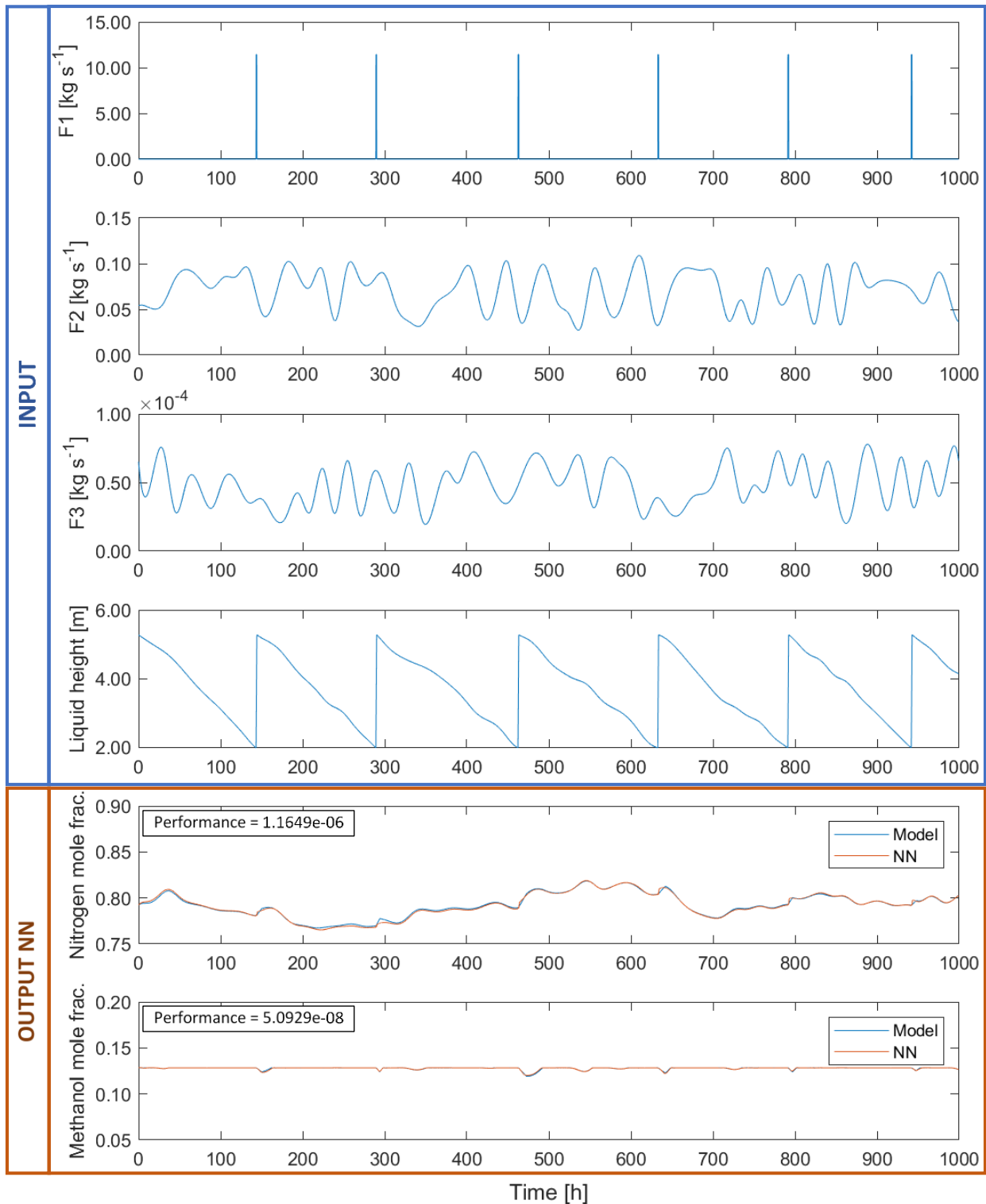


Figure 3.17: Concentration of nitrogen and methanol predicted by setup B when the input showed is presented to the network.

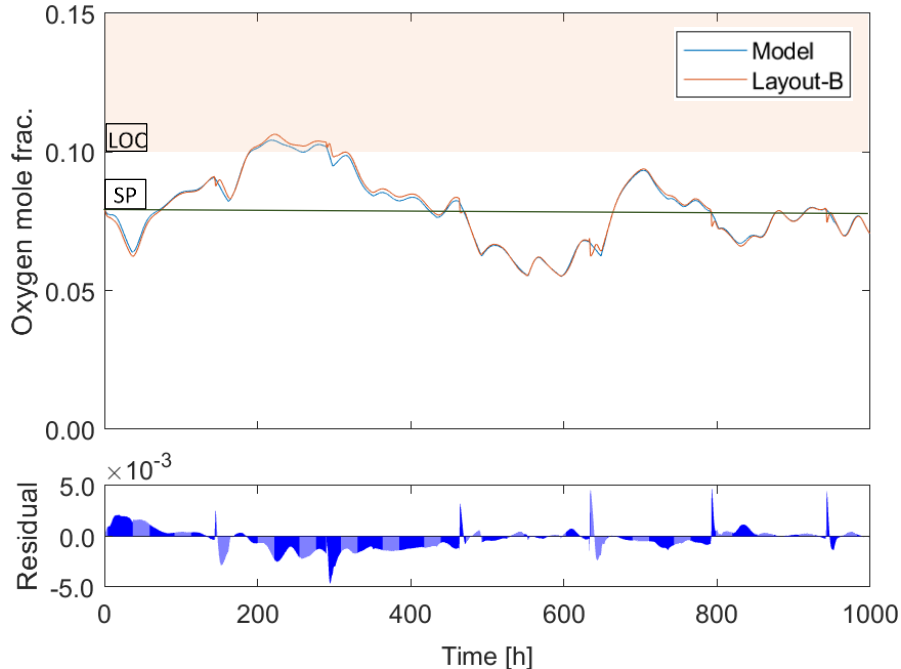


Figure 3.18: Concentration of oxygen calculated from the prediction of the neural network.

3.5. Final Remarks

The tank under consideration provides the methanol required for the operation of the plant's production process. As time goes by, the amount of liquid inside the tank decreases, generating an expansion of the gases in the headspace and a consequent decrease in pressure. Under normal operating conditions the flow of nitrogen maintains the system at atmospheric pressure. However, due to failures in the nitrogen supply system, blockages in the feed pipes or damage of the valves, the nitrogen flow can be reduced or interrupted, then, the pressure inside the system decreases until the setpoint of the vent valve is reached, and the air is allowed to enter. In these situations, the pressure inside the system decreases until reaching the setpoint of the vent valve, and air is allowed to enter. As air intake is permitted, the oxygen concentration inside the tank increases, and if the time is long enough, it may exceed the maximum allowable limit (LOC), verifying the flammability conditions. As evidenced in section 3.1, the increase in the oxygen concentration generated by a decrease in the nitrogen flow does not occur instantaneously, but presents a gradual increase over time, knowing the time it takes for the system to reach the flammability risk conditions allows to continue with the safe operation of the plant until the nitrogen flow is reestablished.

It was possible to obtain a soft sensor capable of predicting the flammability conditions inside a methanol fuel tank. The final configuration was chosen from a set of different configurations. The training of the neural network was done with the mathematical model of the tank.

One of the limitations of the soft sensor developed is that it was obtained using a very simplified mathematical model, in real life the tank is composed of more parts, in addition there are also heat transfer phenomena that modify the behavior of the system. However, by means of this simplified model it is possible to have an idea of the existing relationship between the system variables, which facilitates the selection of the sensor input and output.

In practical terms, when you want to develop a soft sensor, you resort to the historical data of the process. The larger the data set for the neural network training, the greater the chances that the system will find all the existing relationships between the variables. One of the major advantages of using a mathematical model is the freedom to "play with the system", i.e., it is possible to explore process conditions different from the normal working conditions, allowing to obtain new data sets to train the neural network and improve the sensor predictions in limiting conditions.

The process of defining the network architecture is a trial-and-error task, since there are no pre-established rules to set it, however, some rules of thumb can be found in the literature that make this task a little easier. In this case all the neural networks used consist of a single hidden layer. Usually, a single hidden layer of neurons is enough, however, for challenging problems with complex dynamics it is possible to use more than one layer.

The chosen neural network model NARX, presents the characteristic of being fed with past values of the output, which gives it a high capacity to predict time series data, however, when using the predicted outputs, an error accumulation may occur, it is recommended that when applying this type of network, the actual measured values are periodically entered to keep the error propagation under control.

4. Conclusions.

It was possible to design a soft sensor capable of predicting the concentration inside a methanol storage tank with nitrogen inertization system, the best performance was obtained using as input variables the methanol inlet and outlet flow, the nitrogen flow, and the liquid level inside the tank. The soft sensor uses a Neural-Network-NARX model and was trained using a learning set obtained from the mathematical model.

When developing a phenomenological model that represents a physical system, simplifications are made because not all the information of the system to be represented is always known. The validity of these simplifications is checked when the model is compared with experimental data.

Neural networks differ from phenomenological models because they are mathematical models based on the functioning of the brain and can be trained to model a system without knowing the physical laws behind it. During the training process of a neural network, it adjusts its internal parameters, which allows it to adapt and find the existing relationships between variables. This adaptive feature gives neural networks an advantage over traditional mathematical model.

The application of the results of the present work are limited by the ability of the mathematical model to adequately represent the real system, However, it was possible to find existing relationships between the variables and obtain a working network architecture for the scenario under analysis. If it is desired to use the neural network obtained in a real tank, it must first be re-trained with experimental data.

Among the possible applications of the soft sensor developed in the present work can be found:

- Real-time concentration prediction to improve the tank control system and ensure more efficient nitrogen management.
- Backup sensor to identify errors in the physical sensor measurement.
- Backup sensor when maintenance work is performed, and physical sensor measurements are not available.
- Safety alarm, the soft sensor can be used to activate a safety alarm to alert operators of the formation of explosive atmospheres inside the tank.

The procedure used in the present work to obtain the soft sensor is versatile and can be applied in many different applications and equipment, especially in those where experimentation with real devices is not possible due to safety or economic limitations.

It is proposed as future work to improve the mathematical model including all the dynamics of mass and heat transfer within the system, testing the methodology on more complex tank's layouts and if possible, training the neural network with experimental data.

References

American Petroleum Institution (1998) *API 2000: Venting Atmospheric and Low-Pressure Storage Tanks*. 5th edn, *API STANDARD 2000*. 5th edn.

Baldissin, M. (2015) *Misure per prevenire la formazione di atmosfere esplosive*, ASL Milano. Available at: <http://www.asl.milano.it> (Accessed: 5 June 2021).

Bechtold, R. (1997) 'Storage and Dispensing', in *Alternative Fuels Guidebook - Properties, Storage, Dispensing, and Vehicle Facility Modifications*. Available at: <https://app.knovel.com/hotlink/pdf/id:kt006PL6X1/alternative-fuels-guidebook/storage-dispensing-methanol>.

Billings, S.A. (2013) *Nonlinear System Identification*. John Wiley & Sons. doi:10.1002/9781118535561.ch2.

Boussaada, Z. et al. (2018) 'A nonlinear autoregressive exogenous (NARX) neural network model for the prediction of the daily direct solar radiation', *Energies*, 11(3). doi:10.3390/en11030620.

Brett, L. (2015) 'Black Box Methods - Neural Networks and Support Vector Machines.', in *Machine Learning with R*. 2nd edn. Cham: Packt Publishing, pp. 219–257. Available at: <https://app.knovel.com/hotlink/pdf/id:kt0113PJX2/machine-learning-with/black-box-methods-neural>.

Brooks, M.R. and Crowl, D.A. (2007) 'Flammability envelopes for methanol, ethanol, acetonitrile and toluene', *Journal of Loss Prevention in the Process Industries*, 20(2), pp. 144–150. doi:10.1016/j.jlp.2007.01.001.

Carson, P. and Mumford, C. (2002) 'Flammable chemicals', *Hazardous Chemicals Handbook*, pp. 178–227. doi:10.1016/b978-075064888-2/50007-4.

Casal, J. (2008) 'Chapter 3 Fire accidents', *Industrial Safety Series*, pp. 61–117. doi:10.1016/S0921-9110(08)80005-5.

CEN (2006) *Guidance on Inerting for the Prevention of Explosions*. Brussels.

Chang, J.I. and Lin, C.C. (2006) 'A study of storage tank accidents', *Journal of Loss Prevention in the Process Industries*, 19(1), pp. 51–59. doi:10.1016/j.jlp.2005.05.015.

Coker, A.K. (2010) *Ludwig's Applied Process Design for Chemical and Petrochemical Plants*. 4th edn. Available at: <https://app.knovel.com/hotlink/toc/id:kpLAPDCPP1/ludwigs-applied-process/ludwigs-applied-proces>.

Crowl, D.A. and Louvar, J. (2011) 'Chemical process safety: fundamentals with applications', in *Journal of Loss Prevention in the Process Industries*. 2nd edn. Pearson Education. doi:10.1016/s0950-4230(02)00056-6.

Dalena, F. et al. (2018) 'Methanol Production and Applications: An Overview', in *Methanol: Science and Engineering*. Elsevier, pp. 3–28. doi:10.1016/B978-0-444-63903-5.00001-7.

Dewey Johnson (2012) *Global Methanol Market Review*.

European Chemicals Agency (2017) *Guidance on the Application of the CLP Criteria*.

Available at: <https://echa.europa.eu/>.

Fortuna, L. et al. (2001) *Soft Computing*. London: Springer. doi:10.1007/978-1-4471-0357-8.

Fortuna, L. et al. (2007) *Soft Sensors for monitoring and control of industrial processes, Advances in industrial control*. Springer.

Gurney, K. (1997) *An Introduction to Neural Networks*. London: UCL Press.

Haykin, S. (2009) *Neural networks and learning Machine*. Third Edit. Pearson Education.

JOIFF (2015) *Guideline on inerting vertical storage tanks.*, *International Organisation for Industrial Emergency Services Management*. Available at: <https://joiff.com/> (Accessed: 10 June 2021).

Mas, J.F. and Flores, J.J. (2008) 'The application of artificial neural networks to the analysis of remotely sensed data', *International Journal of Remote Sensing*, 29(3), pp. 617–663. doi:10.1080/01431160701352154.

Mashuga, C. V. and Crowl, D.A. (1998) 'Application of the Flammability Diagram for Evaluation of Fire and Explosion Hazards of Flammable Vapors', *Process Safety Progress*, 17(3), pp. 176–183. doi:10.1002/prs.680170305.

Methanex (2006) *Technical Information & Safe Handling Guide for Methanol*, *Methanex Corporation*.

Methanol Institute (2012) *Atmospheric Above Ground Tank Storage of Methanol*. Available at: [http://www.methanol.org/getattachment/Health-And-Safety/Technical-Bulletins/AtmosphericAboveGroundTankStorageMethanol-\(1\).pdf.aspx](http://www.methanol.org/getattachment/Health-And-Safety/Technical-Bulletins/AtmosphericAboveGroundTankStorageMethanol-(1).pdf.aspx) (Accessed: 6 June 2021).

Methanol Institute (2017) *Nitrogen Blanketing for Methanol Storage and Transportation, Methanol safe handling. Technical bulletin*. Available at: <https://www.methanol.org/> (Accessed: 17 June 2021).

NIST (no date) *NIST chemistry WebBook*. doi:10.5860/choice.43sup-0293.

Nyce, D.S. and Lipták, B.G. (2005) 'Inert gas blanketing controls', *Instrument Engineers Handbook, Fourth Edition: Process Control and Optimization*, 2(2005), pp. 2025–2031.

Ott, J. et al. (2012) 'Methanol', in *Ullmann's Encyclopedia of Industrial Chemistry*. Wiley, pp. 1–27. doi:10.1002/14356007.a16_465.pub3.

Pouyakian, M. et al. (2021) 'A comprehensive approach to analyze the risk of floating roof storage tanks', *Process Safety and Environmental Protection*, 146, pp. 811–836. doi:10.1016/j.psep.2020.11.051.

Tauseef, S.M. et al. (2018) 'Case studies of 28 major accidents of fires/explosions in storage tank farms in the backdrop of available codes/standards/models for safely configuring such tank farms', *Process Safety and Environmental Protection*, 120, pp. 331–338. doi:10.1016/j.psep.2018.09.017.

Taveau, J. (2011) 'Explosion of fixed roof atmospheric storage tanks, part 1: Background and review of case histories', *Process Safety Progress*, 30(4), pp. 381–392. doi:10.1002/prs.10459.

Zhen, X. and Wang, Y. (2015) 'An overview of methanol as an internal combustion engine

fuel', *Renewable and Sustainable Energy Reviews*, 52, pp. 477–493.
doi:10.1016/j.rser.2015.07.083.

Zheng, B. and Chen, G. (2011) 'Storage tank fire accidents', *Process Safety Progress*, 30(3), pp. 291–293. doi:10.1002/prs.10458.

Zulkeflee, S.A. and Aziz, N. (2009) *NARX-Model-Based control (NARX-MBC) for citronellyl laurate esterification reactor*, *Computer Aided Chemical Engineering*. Elsevier Inc. doi:10.1016/S1570-7946(09)70652-2.

List of symbols and abbreviations

List of symbols.

Symbol	Definition
u	Input signals
b	Bias
ω	Synaptic weights
ϕ	Activation Function
v	Activation potential
y	Neuron output
α	Momentum constant
η	Learning rate
δ	Local gradient
F_1	Inlet stream of pure liquid methanol
F_2	Outlet stream of pure liquid methanol
F_3	Inlet stream of pure gas nitrogen
F_4	Inlet stream of air
F_5	Outlet stream of vapors
N^L	Total number of moles in liquid phase
N^V	Total number of moles in vapor phase
N_1	Total molar flow to vessel stream 1
N_2	Total molar flow to vessel stream 2
N_3	Total molar flow to vessel stream 3
N_4	Total molar flow to vessel stream 4
N_5	Total molar flow to vessel stream 5
A	Cross sectional area
\emptyset	Molar flux of methanol from liquid to vapor
N_{Nit}^V	Number of moles of nitrogen in vapor phase
N_{Oxy}^V	Number of moles of oxygen in vapor phase
N_{Met}^V	Number of moles of methanol in vapor phase
$y_{4,Oxy}$	Mole fraction of oxygen in air
$y_{4,Nit}$	Mole fraction of nitrogen in air
y_{Nit}	Mole fraction of nitrogen in vapor phase
y_{Oxy}	Mole fraction of oxygen in vapor phase
y_{Met}	Mole fraction of methanol in vapor phase
k_{Met}^V	mass transfer coefficient for methanol
y_{Met}^*	saturation mole fraction of methanol
P_{Met}^*	saturation pressure of methanol
P	pressure of the vessel
V_{tot}	vessel volume
V^L	volume of liquid phase
V^V	volume of vapor phase

ρ	liquid density
MW_{Met}	molecular weight of methanol
MW_{av}	average molecular weight of vapor phase
MW_{Nit}	molecular weight of nitrogen
MW_{Oxy}	molecular weight of oxygen
MW_{Air}	molecular weight of air
R	universal gas constant
T	temperature of the system

List of abbreviations.

LFL	Lower flammability limit
UFL	Upper flammability limit
PRV	Pressure reducing valve
DCS	Digital control system
LOC	Limiting oxygen concentration
MAOC	Maximum allowable oxygen concentration
TP	Trip point
SP	Set point
MSE	Mean square error
ANN	Artificial neural networks
NN	Neural networks
BP	Backpropagation
ARX	Auto-regressive models with exogenous inputs
NARX	nonlinear ARX

Acknowledgments

I would like to thank mainly my parents, Inder and Inés, without their support and effort none of this would be possible; my siblings Jorge and Isabela who are my driving force to keep going every day; my aunts Dora, Done, Lucy, Edilma, Nelly and Lala who have always been there in my difficulties and supporting all my crazy ideas.

To all the people I have met along my way, friends, teachers, colleagues. Special thanks to Jobsan, my partner in adventure, my best advisor, the one who knows how to put my feet on the ground and who was there by my side during the whole process. ¡Juntos lo logramos!

Finally, I thank Professors D. Fissore, M. Demichela and G. Baldissoni for their support, not only in the development of this work, but also in the difficulties encountered along the way. Thank you for your patience and encouragement.

Appendix A: Matlab code - Creation and training NARX Neural network.

```
%Load Learning set
load test_B.mat
X = test_in_B;
T = test_out_yNit;

% Definition of network Architecture
inputDelays = 1:3;
feedbackDelays = 1:3;
hiddenLayerSize = [21];

% Creation of open network
net = narxnet(inputDelays,feedbackDelays,hiddenLayerSize,'open');
    % Choose Input and Feedback Pre/Post-Processing Function
net.inputs{1}.processFcns = {'mapminmax'};
net.inputs{2}.processFcns = {'mapminmax'};
net1.layers{1}.transferFcn='logsig';           % Transfer function hidden layer
net1.layers{2}.transferFcn='purelin';         % Transfer function output layer

% Define training algorithm
trainFcn = 'trainlm';                         % Levenberg-Marquardt
backpropagation.
net.trainParam.epochs = 100;                  % Maximum number of epochs to train
net.trainParam.goal = 0;                      % Performance goal
net.trainParam.max_fail = 6;                  % Maximum validation failures
net.trainParam.min_grad = 1e-7;              % Minimum performance gradient
net.trainParam.mu = 0.001;                   % Initial mu
net.trainParam.mu_dec = 0.1;                 % mu decrease factor
net.trainParam.mu_inc = 10;                  % mu increase factor
net.trainParam.mu_max = 1e10;                % Maximum mu
net.trainParam.time = inf;                   % Maximum time to train in seconds
net.performFcn = 'mse';                       % Mean Squared Error

% Prepare the Data for Training and Simulation of the open network
[x,xi,ai,t] = preparets(net,X,{},T);

% Setup Division of Data for Training, Validation, Testing
net.divideFcn = 'dividerand';                 % Divide data random
net.divideMode = 'time';                     % Divide up every sample
net.divideParam.trainRatio = 70/100;
net.divideParam.valRatio = 15/100;
net.divideParam.testRatio = 15/100;

% Train the Open-Network
[net,tr] = train(net,x,t,xi,ai);

% Test the Network
y = net(x,xi,ai);
e = gsubtract(t,y);
performance = perform(net,t,y)

% Conversion of open to close Network
```

```

netc = closeloop(net);
netc.name = [net.name ' - Closed Loop'];

% Define training algorithm
netc.trainFcn = 'trainlm'; % Levenberg-Marquardt
backpropagation.
netc.trainParam.epochs = 100; % Maximum number of epochs to
train
netc.trainParam.goal = 0; % Performance goal
netc.trainParam.max_fail = 6; % Maximum validation failures
netc.trainParam.min_grad = 1e-7; % Minimum performance gradient
netc.trainParam.mu = 0.001; % Initial mu
netc.trainParam.mu_dec = 0.1; % mu decrease factor
netc.trainParam.mu_inc = 10; % mu increase factor
netc.trainParam.mu_max = 1e10; % Maximum mu
netc.trainParam.time = inf; % Maximum time to train in seconds
netc.performFcn = 'mse'; % Mean Squared Error

% Prepare the Data for Training and Simulation of the closed network
[xc,xic,aic,tc] = preparets(netc,X,{},T);

% Setup Division of Data for Training, Validation, Testing
netc.divideFcn = 'dividerand'; % Divide data random
netc.divideMode = 'time'; % Divide up every sample
netc.divideParam.trainRatio = 70/100;
netc.divideParam.valRatio = 15/100;
netc.divideParam.testRatio = 15/100;

% Train the Open-Network
[netc trc Ycs Ecs Xcf Acf ] = train(netc,xc,tc,xic,aic);

%Test the close-Network
yc = netc(xc,xic,aic);
closedLoopPerformance = perform(net,tc,yc)

%Save the Network
save Closed_NeuralNetwork netc

```

Appendix B: Matlab code - Input Random Generation

```
%Random Vector Generation
samp_time = 10;           % [s] Sampling time in seconds
periodicity = 90;        %
n_points = 10000;        % Number of dataset points
F2_ss = 0.0680866402;    % [kg s-1] F2 stationary value
F3_ss = 6.2e-5;          % [kg s-1] F3 stationary value
F2_range = 0.2;          % Max amplitude of variation in F2
F3_range = 0.2;          % Max amplitude of variation in F3

ts = samp_time*60;        % [s] Sampling time in seconds
t_tot = ts*(n_points);    % [s] Simulation time

F2_min = F2_ss*(1-F2_range); % [Kg s-1] Min value for F2
F2_max = F2_ss*(1+F2_range); % [Kg s-1] Max value for F2
F3_min = F3_ss*(1-F3_range); % [Kg s-1] Min value for F3
F3_max = F3_ss*(1+F3_range); % [Kg s-1] Max value for F3

t = [];
t(1) = 0;
i=1;

% Random Vector time generation
while t(i) < t_tot
    i = i+1;
    t(i) = t(i-1) + periodicity*ts + periodicity/5*ts*rand;
end

% Random Vector input variables generation
for i=1:length(t)
    coeff_1 = rand;
    coeff_2 = rand;
    coeff_3 = rand;
    coeff_4 = rand;

    if coeff_1<=0.5
        coeff_1 = -1;
    else
        coeff_1 = 1;
    end

    if coeff_3<=0.5
        coeff_3 = -1;
    else
        coeff_3 = 1;
    end

    F2(i) = F2_ss*(1+coeff_1*coeff_2*F2_range);
    F3(i) = F3_ss*(1+coeff_3*coeff_4*F3_range);

    clear coeff_1 coeff_2 coeff_3 coeff_4
end

% Resampling
```

```
t_sampled = [0:ts:t(end)];  
t_sampled((n_points+1):end) = [];  
F2_sampled = spline(t,F2,t_sampled);  
F3_sampled = spline(t,F3,t_sampled);  
  
% Rescaling  
F2_scale = rescale(F2_sampled,F2_min,F2_max);  
F3_scale = rescale(F3_sampled,F3_min,F3_max);  
  
RandomVector = [t_sampled' F2_scale' F3_scale'];
```